



# Continuous atmospheric CO<sub>2</sub>, CH<sub>4</sub> and CO measurements at the OPE station in France from 2011 to 2018

Sébastien Conil<sup>1</sup>, Julie Helle<sup>2</sup>, Laurent Langrene<sup>1</sup>, Olivier Laurent<sup>2</sup>, Michel Ramonet<sup>2</sup>

<sup>1</sup>DRD/OPE, Andra, Bure, 55290, FRANCE

5 <sup>2</sup> Laboratoire des Sciences du Climat et de l'Environnement (LSCE/IPSL), UMR CEA-CNRS-UVSQ, Gif-sur-Yvette, France

*Correspondence to:* Sébastien Conil ([sebastien.conil@andra.fr](mailto:sebastien.conil@andra.fr))

**Abstract.** Located in the North East of France, the Observatoire Pérenne de l'Environnement (OPE) station was built during the Integrated Carbon Observation System (ICOS) Demonstration Experiment to monitor the atmospheric concentration of greenhouse gases. Its continental rural background setting allows to fill the gaps between oceanic or mountain background stations and urban stations within the ICOS network. Continuous measurements of several greenhouse gases using high precision spectrometers started in 2011 on a tall tower with three sampling inlets at 10m, 50m and 120m above the ground. The measurements quality are regularly assessed using several complementary approaches based on reference high pressure cylinders, traveling instruments audit and sets of travelling cylinders (so-called cucumber intercomparison). Thanks to the quality assurance strategy recommended by ICOS, the measurements precision are within the WMO compatibility goals for carbon dioxide (CO<sub>2</sub>), methane (CH<sub>4</sub>) and carbon monoxide (CO). The mixing ratios time series from 2011 to end of 2018 allow analyses of trends and diurnal and seasonal cycles. The CO<sub>2</sub> and CH<sub>4</sub> annual growth rates are respectively 2.4 ppm/year and 8.8 ppb/year for the 120m above ground measurements over the investigated period. No significant trend has however been recorded for the CO mixing ratios. The afternoon mean residuals of these three compounds are significantly stronger during the cold period when inter-species correlations are high, compared to the warm period. The residuals variabilities show a close link with the air masses back-trajectories.

## 1 Introduction

Since the beginning of the industrial era, atmospheric concentration of long lived greenhouse gases (GHG) are rising. Increases in the surface emissions, mostly from human activities, are responsible for this atmospheric GHG build up. For carbon dioxide (CO<sub>2</sub>), the largest climate change contributor, only nearly half of the additional anthropogenic emissions are retained in the atmosphere, the remaining 50% being pumped out by the ocean and the land ecosystems (Le Quéré et al., 2018). Regarding the methane (CH<sub>4</sub>) the last 10 years are characterized by high growth rates at many sites, following a period of stable concentrations from 2000 to 2007 (Nisbet et al., 2019; Turner et al., 2019). Monitoring the atmospheric concentrations of those GHG's is of primary importance for the long-term climate monitoring but also for the surface fluxes assessment. Remote and mountain atmospheric measurements, because they are performed far from anthropogenic sources and/or are located in the



free troposphere, are necessary to assess the background concentrations. Such « global scale » data are of great value to monitor the global atmospheric GHG build-up but also to estimate global scale fluxes. However, they are not designed to capture regional-scale signals necessary to assess local to regional scale fluxes. The European Integrated Carbon Observation System (ICOS) precisely aims at establish and maintain a dense European GHG observations network to monitor long-term changes, assess the carbon cycle and track carbon and GHG fluxes. Atmospheric inverse methods combining tall tower network measurements and transport models are great tools to assess the surface GHG fluxes exchanged with biosphere and oceans, and to estimate the anthropogenic emissions (Broquet et al., 2013 ;Kountouris et al., 2018). They also offer independent ways to improve the bottom-up emissions inventories required by the international agreement under UNFCCC (Bergamaschi et al., 2018; Leip et al., 2018; Peters et al., 2017).

10 ICOS was established as a European strategic research infrastructure which will provide the high precision observations needed to quantify the greenhouse gas balance of Europe and adjacent regions. It is now a distributed infrastructure composed of three integrated networks measuring GHG in the atmosphere, over the ocean and at the ecosystem level. Each network is coordinated by a thematic center that performs centralized data processing. One of the key focuses of ICOS is to provide standardized and automated high-precision measurements, which is achieved by using common measurement protocols and standardized instrumentations. During the preparatory phase from 2008-2013 a demonstration network and new stations were set up with harmonized specifications (Laurent et al ; 2017). The Atmospheric Thematic Center (ATC) performs several metrological tests on the analysers as well as technical support and training regarding any aspects of the in situ GHG measurements (Yver Kwok et al., 2015). The ATC is also responsible of the near real time post processing of the measurements (Hazan, et al., 2016).

20 The OPE station was established as a close collaboration between Andra and LSCE in the framework of the demonstration experiment during 2010 and 2011 following the ICOS atmospheric station specifications. It is a continental regional background station contributing to the actual network by bridging the gap between remote global/mountain station like Mace Head or Jungfrauoch, and urban stations like Saclay or Heidelberg. The potential of ICOS continuous measurements of CO<sub>2</sub> dry air mole fraction to improve Net Ecosystem Exchange estimates at the mesoscale across Europe has been evaluated in Kadygrov et al. (2015). Pison et al. (2018) addressed the potential of the actual ICOS European network for the methane emission estimation at the French national scale.

25 The main objectives of this paper are to describe the OPE monitoring station, the measurements system, to present its performance and to draw some results from the first 8 years of continuous operations.

## 2 Site description and GHG measurements system

### 2.1 Site location

30 The OPE atmospheric station (48.5625°N, 5.50575°E WGS84, 395 m asl) is located on the eastern edge of the Paris Basin in the North East part of France, western Europe, as shown on Figure 1. The landscape consists of undulated eroded limestone plateaux dissected by a few SE-NW valleys (60 to 80m). The station is on top of the surrounding hills in a rural area with large



crop fields, some pastures and forest patches. The dominating land cover types according to Corine Land Cover 2012 in the 25 / 100 km surroundings are Arable land/crops: 39% /44%, Pastures : 14% /18%, Forest : 44% /34%. The mean population density within a 25 / 100km radius from the station based on GEOFLA database from Institut national de l'information géographique et forestière (IGN) are 26 / 64 (inhab.km<sup>-2</sup>). The closest small towns are Delouze with 130 people located 1 km at the SE and Houdelaincourt with 300 people located 2km at the SW. The closest cities are Saint Dizier (45 000 inhabitants) located 40km away at the W, Bar Le Duc (35 000 inhab.) 30km at the NW, Toul (25 000 inhab.) 30km at the E and Nancy (450 000 inhab.) 50km at the E. The major road with 20 000 cars/day is located 15km to the North (RN4). The station includes a 120m tall tower and two portable and modular buildings fully equipped on a 2ha fenced area. The station infrastructures were built in 2009 and 2010 and the measurements systems started in 2011.

5

10 The OPE station is designed to host a complete set of in situ measurements of meteorological parameters, trace gases (CO<sub>2</sub>, CH<sub>4</sub>, N<sub>2</sub>O, CO, O<sub>3</sub>, NO<sub>x</sub>, SO<sub>2</sub>) and particles parameters(size distribution, absorption and diffusion coefficients, number and mass, chemical composition, radioactivity). The station is part of the French aerosol in situ network contributing to ACTRIS and AERONET program. It is part of the IRSN (Institut de Radioprotection et de Sûreté Nucléaire) network for the ambient air radioactivity monitoring. The station is also contributing to the french air quality monitoring network and to the European

15 Monitoring and Evaluation Program.



**Figure 1: Geographical location of the OPE atmospheric station (left panel) and aerial photograph illustrating the landscape surrounding the station (right panel).**

## 2.2 Local meteorology and air masses trajectories

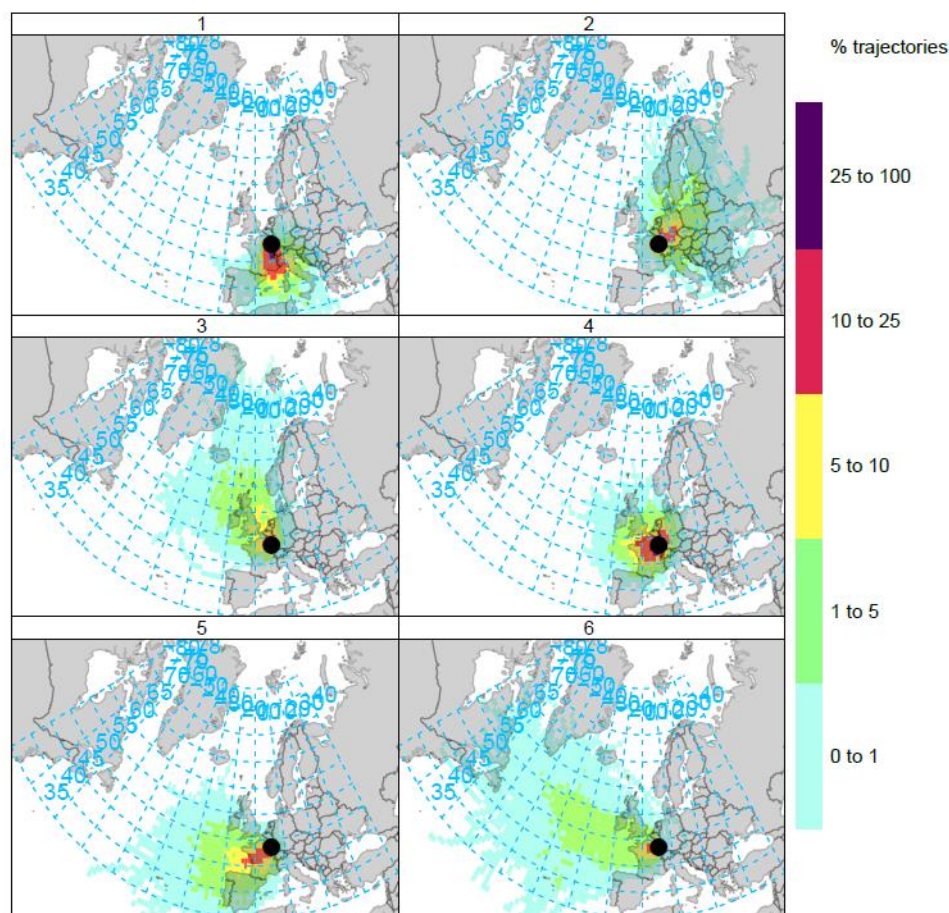
20 The local meteorology is monitored using three sets of meteorological sensors located at the three measurement levels on the tower (10m, 50m and 120m agl). Standard meteorological parameters, Temperature, Relative Humidity, Pressure and Wind Speed and Direction, are monitored in compliance with the ICOS AS specifications. Minute averaged data are logged and used to produce hourly mean fields. In addition there is a ground based weather station operated by Meteo France, the French



national weather service providing hourly mean data in compliance with the World Meteorological Organization specifications.

The mean annual temperature over the period 2011-2018 is around 10.5°C. The minimum temperature was -15,2°C and the maximum temperature was 36.4°C. The cumulated annual precipitations are on average 829mm. Two local wind regimes are predominant, a south/westerly regime and an easterly/north easterly regime.

96h back trajectories were computed for the OPE station top level (120m) using the NCEP reanalysis fields and HYSPLIT model every 6 hours. As we focus on the afternoon mean residuals, we use only back-trajectories reaching the OPE station at 12:00 UTC. The clustering tools from HYSPLIT was used to determine the main air masses type reaching the station. Six clusters were defined as shown on the Figure 2. This figure shows the frequency of trajectories for each cluster passing through the corresponding grid point and reaching the OPE station at 12:00 UTC. Clusters 1 to 3 are characterized by continental air masses type. Cluster 4 is dominated by slow moving trajectories from the western part. Cluster 5 and 6 are dominated by western marine trajectories.



15 **Figure 2: 96h back-trajectory frequencies reaching the OPE station top level for each of the 6 clusters identified using the HYSPLIT tools and the NCEP reanalysis for the period 2011-2018.**



### 2.3 GHG measurements system

The GHG measurements system was setup in 2011 with support from the ICOS Preparatory Phase projects. It was built in order to comply with the Atmospheric Station class 1 stations specifications from ICOS. It relies on a fully automated samples distribution system with remote control backed up by an independent robust spare distribution system. It includes several  
5 continuous analysers for the main GHG CO<sub>2</sub>, CH<sub>4</sub> and N<sub>2</sub>O, a manual flask sampler as well as specific analysers or samplers for tracers such as radon, CO and <sup>14</sup>CO<sub>2</sub>.

The continuous GHG measurements system is made of three main parts: an ambient air samples preparation and distribution component, a reference gases distribution component and a master component which is conducting the main analysis sequence and controlling the distribution and analysis systems through pressure and flowrate meters. The stations flow diagram is  
10 described on the Figure 3. The ambient air is collected at three levels on the tower at 10m, 50m and 120m levels and brought down to the shelter located at the tower base using 0.5 inches outer diameter Dekabon tubings equipped with a stainless steel inlet designed to excludes precipitations. Five sampling lines are installed at 120m, and three are installed at 10m and 50m. From the 120m level, one line is connected to the <sup>14</sup>CO<sub>2</sub> sampler built by the Heidelberg University. Another sampling line is used to collect weekly flask samples. The continuous GHG measurements are done using two independent sampling lines. The  
15 last line is a spare line which can be operated in case of trouble on one line or in case of temporary additional experiments such as independent audit as the ones performed in 2011 or 2014. At 10m and 50m levels, two lines are used for the continuous GHG measurement system. Another spare line is also installed for each of the 10m and 50m level.

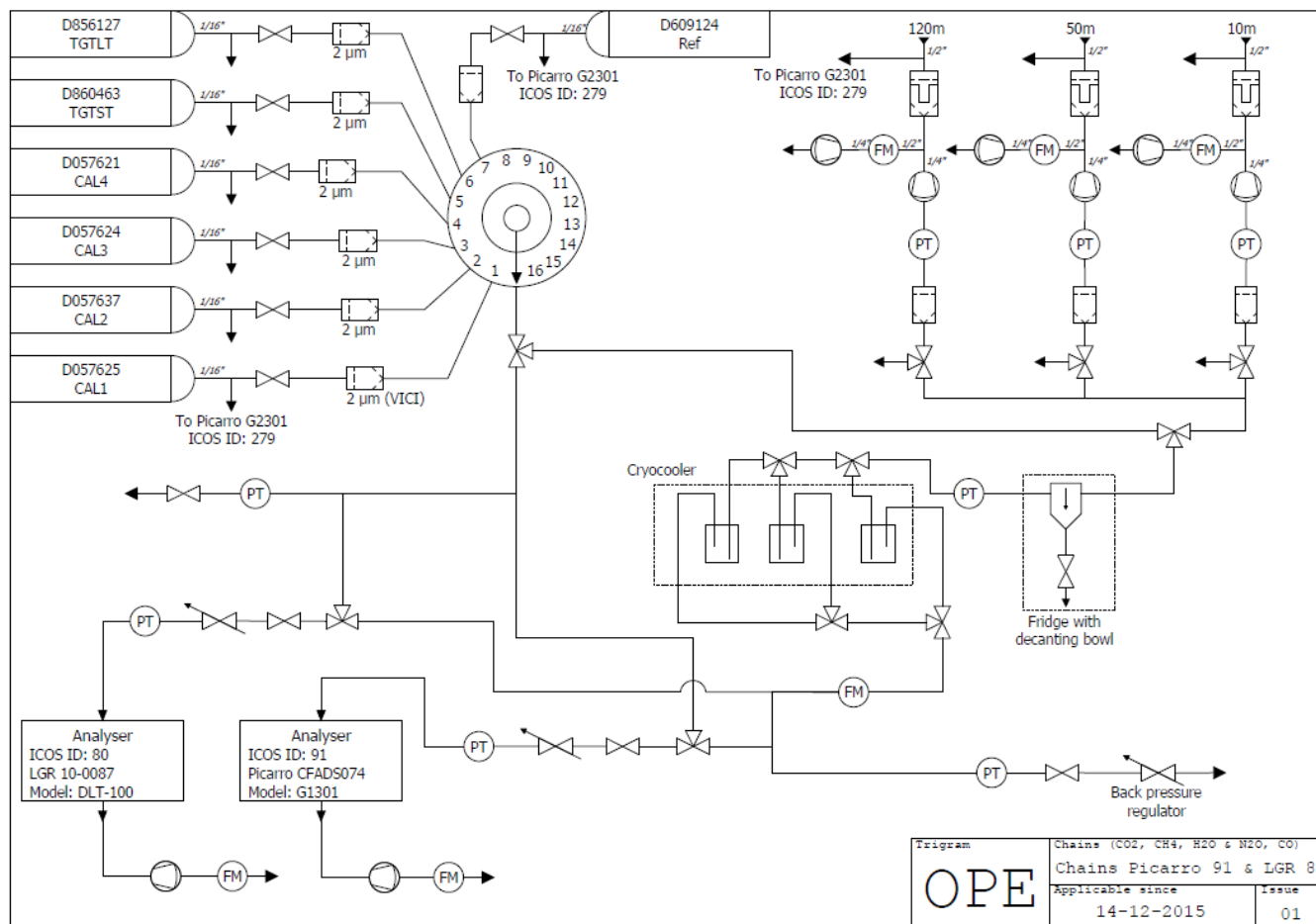
At each level, the continuous GHG monitoring system air is flushed from the tower using three flushing pumps Neuberger N815KNE (15 LPM nominal flow rate) and cleaned by a couple of 40 microns and 7 microns Swagelok stainless steel filters.  
20 From each sampling line, a secondary pump KNF N86KTE-K (5.5 LPM nominal flow rate) is used to sample and pressurize (through a 2 micron Swagelok filter) the air to be dried and then analysed. A flowmeter is used to monitor the air flow in the flushing line and a pressure sensor is used to monitor the sampling line pressure. The air sample is pre-dried by a fridge through a coil (to increase the path in the fridge and the residence time). To further dry the sample, the air passes through a 335mL glass trap cooled in an ethanol bath at -50°C using a dewar. Once dried in the cryo water traps (-40°C dew point), the air  
25 sample is pressure regulated (~1150 hPa abs at the instrument inlet) and brought to the analysers.

The ambient air distribution component is driven by a control control/command component, designed around a Programmable Logic Controller (PLC), which is dedicated to the selection and distribution of the ambient air sample from the three sampling heights. This distribution component selects an ambient air sample from one of the three levels using three 3-ways solenoid valves and then route it to the drying system and then to the air analysers. Once analysed, the air sample flows back to the  
30 distribution panel where a backward pressure regulator controls the air pressure in the sample line. A pressure sensor monitors the pressure at the analyser inlets and a flow meter monitors the flow rate at the analyser outlets.

The control/command component system selects between standards and ambient air, following the PLC's order, the PLC being responsible of the sequence management and quality control processes. The standard gas distribution component is based on



a 16 position Vici Valco valve from which nine ports are connected to the analysers. The pressure of the selected standard gas or the ambient air sample is adjusted at the analyser inlet by a manual pressure regulator. All the distributing tubings are stainless steel either 1/8 or 1/4 inches and are over pressurized to avoid any leakage artifact. According to ICOS internal rules, global leakage checks are performed on a yearly basis and after any maintenance operation



5

**Figure 3: Flow diagram of the OPE GHG measurement system**

The analysers used are Picarro cavity ring down spectrometers (CRDS) series G1000 and G2000 for CO<sub>2</sub>, CH<sub>4</sub>, H<sub>2</sub>O and CO and Los Gatos Research Off-Axis-ICOS-spectrometers for N<sub>2</sub>O and CO. Each analyser used at the station went first through extensive lab tests at LSCE during the development of the ICOS Metrology lab at ATC (Lebague et al., 2016, Yver Kwok et al., 2015). These initial tests provide valuable informations about the intrinsic properties of the analysers, their precision, stability, water vapour sensitivity and temperature dependence.

10



Over the period 2011-2018 the reference analysers are a Picarro G1301 (ICOS# 91) which performs CO<sub>2</sub> and CH<sub>4</sub> (and H<sub>2</sub>O) mole fractions analysis and a Los Gatos DLT100 (ICOS #80) is used for CO (and H<sub>2</sub>O) mole fraction measurement. A couple of spare and parallel instruments have been running either on the principal distribution system and /or on the spare distribution system following the same calibration and quality control strategy.

5 The calibrations strategy includes four consecutive cycles of the four calibration cylinders sampled for 30 minutes each, the complete calibration lasts 8 hours. An archive reference standard gas nicknamed Long Term Target (LTT) is injected every 2 or 3 weeks for a duration of 30 minutes while a common archive reference standard gas nicknamed Short Term Target (STT) is injected for 20 minutes every 10 hours. Another short term working standard nicknamed Reference (REF) gas is also used every 10 hours to correct the short term variability. The concentrations of the standards were defined following the ICOS  
10 specifications (Laurent, 2017). The standard gases are supplied using SCOTT Nickel-plated brass regulator from 50l Luxfer Aluminium cylinder. Before march 2016, the standard and performance cylinders used were prepared by LSCE and were traceable to WMO scales (CO<sub>2</sub>:WMOX2007, CH<sub>4</sub>: WMOX2007, CO: WMO-CO-X2014, N<sub>2</sub>O: WMOX2007). Since march 2016, the standard and performance cylinders used have been prepared by the CAL of ICOS and are traceable to WMO scales (CO<sub>2</sub>:WMOX2007, CH<sub>4</sub>: WMO-2004, CO: WMO-CO-X2014, N<sub>2</sub>O: NOAA-2006 ). Short Term Target and Reference  
15 cylinders are refilled every 6 month by the Central Analytical Laboratories of ICOS.

The raw data from the analysers as well as the distribution system monitoring parameters are transmitted to the ATC database on a daily basis. Data is then processed following Hazan et al. (2016) including a specific water vapour correction for the remaining humidity, as well as station specific automatic flagging process. Data products are then generated allowing a regular control of the data quality. Additionally a manual flagging is performed by the station PI on the raw data as well as on the  
20 hourly aggregated data.

The routine operating sequence includes in a sequence order

- Start with a complete calibration of 4 cycles of 4 standards lasting 8 hours followed by 30min of LTT and then by 30min of STT,
- 5 hours of ambient air in cycles of 3 steps of 20min fo the 10m level, 50m level and then 120m level
- 25 - 20min of REF
- 5 hours of ambient air in cycles of 3 steps of 20min of the 10m level, 50m level and then 120m level
- 20min of STT

During the first years of the ICOS preparatory phase, the calibrations were performed every two weeks. For gas consumption issue and after optimization tests, they are now performed on a 3 weeks basis.

30 The flushing and stabilisation periods for the standards are 10 minutes meaning that the first 10 minutes of data for each standards are rejected. The flushing and stabilisation period for the ambient air samples are 5 minutes meaning that the first 5 minutes of data for each ambient air levels are rejected (only 15min on the total 20minutes every hour are available).The raw data are then calibrated using the 2 weeks or 3 weeks complete calibration and REF working standards following Hazan et al.



(2016). Raw data (between 1s and 5s resolution) are aggregated to minutes and hourly averages. The results presented here are based on validated minute data from mid 2011 to end of 2018.

For  $^{14}\text{C}$  analyses, two-weeks integrated large volume samples of atmospheric  $\text{CO}_2$  are also collected from the 120m inlet by quantitative chemical absorption in basic sodium hydroxide (NaOH) solution, as described by Levin et al. (1980).  $\text{CO}_2$  samples are then processed in the Heidelberg  $^{14}\text{C}$  laboratory by acidification of the NaOH solution in a vacuum system. The extracted  $\text{CO}_2$  is subsequently purified over charcoal. The  $^{14}\text{C}/\text{C}$  ratio is then measured by low level counting (Kromer and Münnich, 1992).

The Table 1 gives an outlook of the different analysers and sensors that were used at the station over different periods.

Parameter	Analyser	ICOS Id	Levels	Frequency	Period 1	Period 1	Period 2	Period 2	Period 3	Period 3	Period 4	Period 4
$\text{CO}_2/\text{CH}_4/\text{H}_2\text{O}$	Picarro G1301	91	10m / 50m /120m	5s/1min/1h	20/07/2011	06/11/2012	18/03/2013	18/05/2017				
$\text{CO}_2/\text{CH}_4/\text{H}_2\text{O}$	Picarro G2301	75	10m / 50m /120m	5s/1min/1h	20/04/2011	07/11/2013						
$\text{CO}_2/\text{CH}_4/\text{CO}/\text{H}_2\text{O}$	Picarro G2401	187	10m / 50m /120m	5s/1min/1h	12/02/2014	24/03/2014	12/05/2014	03/08/2014	04/09/2014	18/12/2015	11/12/2017	24/09/2018
$\text{CO}_2/\text{CH}_4/\text{H}_2\text{O}$	Picarro G2301	379	10m / 50m /120m	5s/1min/1h	27/01/2016	24/11/2017						
$\text{CO}_2/\text{CH}_4/\text{CO}/\text{H}_2\text{O}$	Picarro G4301	728	10m / 50m /120m	5s/1min/1h	24/09/2018	-						
$\text{CO}/\text{N}_2\text{O}/\text{H}_2\text{O}$	Los Gatos Research $\text{N}_2\text{O}$ and CO	80	10m / 50m /120m	1s/1min/1h	13/05/2011	24/11/2017						
$\text{CO}/\text{N}_2\text{O}/\text{H}_2\text{O}$	Los Gatos Research $\text{N}_2\text{O}$ and CO	478	10m / 50m /120m	1s/1min/1h	05/04/2018	-						
Wind	Gill Wind Observer		10m / 50m /120m	5s/1min/1h	05/05/2011							
Temperature - Relative Humidity	Vaisala HMP155A		10m / 50m /120m	5s/1min/1h	05/05/2011							
Pressure	RM Young 61302		10m / 50m /120m	5s/1min/1h	05/05/2011							
Radon monitor	U Heidelberg	117	10m	30 min	25/03/2011	22/08/2011						
Radon monitor	U Heidelberg	118	10m	30 min	16/09/2011	05/01/2012						
Radon monitor	ANSTO	546	120m	30 min	10/07/2017							
Integrated NaOH $^{14}\text{C}$ sampler	U Heidelberg		120m	2 weeks	25/03/2011	-						
Flask sampler	LSCE		120m	1 week	12/05/2011	15/07/2014	27/05/2015					
Mixing layer height	Lidar Leosphere ALS 300			30s/15min	23/04/2011	15/11/2012	18/01/2013	01/04/2013	30/05/2013	30/07/2013	06/12/2013	03/11/2014

10 **Table 1: Analysers, sensors and samplers, atmospheric parameters, associated ICOS reference number as well as the period of operation at the station**

## 2.4 Composite merged time series

The GHG data covers several years and were collected using different sampling systems and analysers. In each of the individual time series, some data are missing because of either sampling issues, analyser's problems or local contaminations near the station. Very local pollutions due, for example to field works, infrastructure maintenance, are very uncommon and occur only rarely. Power outage also happened because of lightings and construction work. Troubles on the sampling systems are more frequent and may include tubing leak, pump troubles, filters clogging or control/command component system failure. Analysers troubles are also quite common and range from software issues, operating system failures, hardware problems (hard disk, fan, ...), or worse, liquid contamination (from water or ethanol) of the optical cell.





From these individual time series, we built three combined time series for CO<sub>2</sub>, CH<sub>4</sub> and CO filling the gaps when possible using only « real » observations (but not using any synthetic data from models). To build these times series from the different analyser's dataset we use the priority order given in Table 2.

Compound	Instrument 1	Instrument 2	Start Date	End Date
CO <sub>2</sub>	75 (Picarro G1301)	-	21/04/2011 00:00	20/07/2011 23:00
CH <sub>4</sub>	75 (Picarro G1301)	-	21/04/2011 00:00	20/07/2011 23:00
CO	80 (Los Gatos CO/N <sub>2</sub> O)	-	12/05/2011 00:00	07/11/2012 00:00
CO <sub>2</sub>	91 (Picarro G1301)	75 (Picarro G1301)	21/07/2011 00:00	05/11/2013 23:00
CH <sub>4</sub>	91 (Picarro G1301)	75 (Picarro G1301)	21/07/2011 00:00	05/11/2013 23:00
CO	80 (Los Gatos CO/N <sub>2</sub> O)	-	11/03/2013 00:00	12/02/2014 00:00
CO <sub>2</sub>	91 (Picarro G1301)	-	06/11/2013 00:00	11/02/2014 23:00
CH <sub>4</sub>	91 (Picarro G1301)	-	06/11/2013 00:00	11/02/2014 23:00
CO	187 (Picarro G2401)	80 (Los Gatos CO/N <sub>2</sub> O)	12/02/2014 00:00	18/12/2015 00:00
CO <sub>2</sub>	91 (Picarro G1301)	187 (Picarro G2401)	12/02/2014 00:00	27/01/2016 00:00
CH <sub>4</sub>	91 (Picarro G1301)	187 (Picarro G2401)	12/02/2014 00:00	27/01/2016 00:00
CO	80 (Los Gatos CO/N <sub>2</sub> O)	-	18/12/2015 00:00	07/12/2017 00:00
CO <sub>2</sub>	91 (Picarro G1301)	379 (Picarro G2301)	27/01/2016 00:00	22/06/2017 00:00
CH <sub>4</sub>	91 (Picarro G1301)	379 (Picarro G2301)	27/01/2016 00:00	22/06/2017 00:00
CO <sub>2</sub>	379 (Picarro G2301)	-	22/06/2017 00:00	14/12/2017 00:00
CH <sub>4</sub>	379 (Picarro G2301)	-	22/06/2017 00:00	14/12/2017 00:00
CO <sub>2</sub>	187 (Picarro G2401)	-	14/12/2017 00:00	03/04/2018 14:00
CH <sub>4</sub>	187 (Picarro G2401)	-	14/12/2017 00:00	03/04/2018 14:00
CO	187 (Picarro G2401)	-	14/12/2017 00:00	05/04/2018 18:00
CO <sub>2</sub>	379 (Picarro G2301)	187 (Picarro G2401)	03/04/2018 14:00	24/09/2018 14:00
CH <sub>4</sub>	379 (Picarro G2301)	187 (Picarro G2401)	03/04/2018 14:00	24/09/2018 14:00
CO	187 (Picarro G2401)	478 (Los Gatos CO/N <sub>2</sub> O)	05/04/2018 18:00	10/09/2018 14:00
CO	187 (Picarro G2401)	478 (Los Gatos CO/N <sub>2</sub> O)	10/09/2018 14:00	24/09/2018 14:00
CO	478 (Los Gatos CO/N <sub>2</sub> O)	-	24/09/2018 14:00	24/09/2018 14:30
CO <sub>2</sub>	379 (Picarro G2301)	-	24/09/2018 14:00	24/09/2018 14:30
CH <sub>4</sub>	379 (Picarro G2301)	-	24/09/2018 14:00	24/09/2018 14:30
CO	728 (Picarro G2401)	478 (Los Gatos CO/N <sub>2</sub> O)	24/09/2018 14:30	17/01/2019 09:59
CO <sub>2</sub>	379 (Picarro G2301)	728 (Picarro G2401)	24/09/2018 14:30	17/01/2019 09:59
CH <sub>4</sub>	379 (Picarro G2301)	728 (Picarro G2401)	24/09/2018 14:30	17/01/2019 09:59

5 **Table 2: Order priority for the CO<sub>2</sub>/CH<sub>4</sub>/CO compounds with ICOS instrument identifiers and associated period**

The different instruments were used in parallel for some time and it is thus possible to assess the systematic differences between the data for these common periods. The instruments may have shared sampling tubes, calibration and quality control gases but may have also used different air distribution system and different cylinders. Consequently, differences may occur due to troubles in time synchronisation, air sampling (sampling and flushing pumps efficiency) , calibration and correction or any other causes not yet identified.

10



5 The Figure 4 shows the mean afternoon (12:00-17:00 UTC) data difference between the different instruments analysing ambient air at the 120m level for CO<sub>2</sub> and CH<sub>4</sub>. Large deviations in the afternoon mean are revealed by such comparison. On average over the full period the differences are -0.002 ppm for CO<sub>2</sub> and -0.27 ppb for CH<sub>4</sub>, below the WMO compatibility goals. These large deviations may come from various uncertainty source, such as residence time difference in the sampling systems, water vapour correction, clock issue, or internal analyser uncertainties.

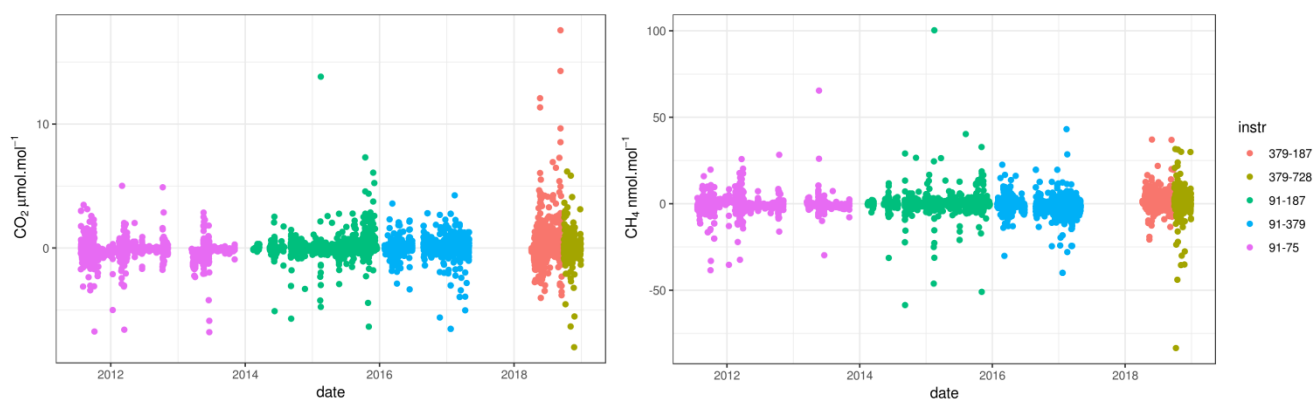


**Figure 4: Difference between hourly mean afternoon (12:00-17:00 UTC) data at the top level 120m from the two instruments used at the same time at the OPE station from 2011 to 2018 for CO<sub>2</sub> (left panel) and CH<sub>4</sub> (right panel). The different instruments couples are shown in colour and their identifiers are labelled in the legend of the right panel.**

10 Schibig et al. (2015) have shown results of the comparison between CO<sub>2</sub> measurements from two continuous analysers run at the Jungfraujoch GAW station in Switzerland. The hourly means of the two analysers showed a general good agreement, with mean differences on the order of 0.04 ppm (with a standard deviation of 0.40ppm). However large deviations of several ppm were also found.

## 2.5 Data processing

15 Raw data from the instruments (mole fractions and internal parameters such as cell temperature/pressure, outlet valve), and from the air distribution system (sequence information and ancillary data such as pressure and flow rates in the sampling lines) are transferred at least once a day to the ATC data server. Data are then processed automatically as described in Hazan et al., (2016). Raw data are flagged using a set of parameters defined for the station and instrument. A manual flag is then applied by the station PI in order to eventually discard data using local station information (e.g. local contamination, maintenance  
20 operation, leakage, instrumental malfunctions, etc...). Corrections related to the water vapour content, and the calibration are then applied. Finally, data are aggregated in time to produce minute, hourly and daily means.

The hourly time series exhibit strong variability from hourly to decennial time scale. These variations may be related to meteorological and climate changes, and to sources and sinks variations. We are mostly interested in the regional signatures at scales that can be approached by the model inversion and assimilation framework. For this reason we want to isolate from



the time series and data aggregation the situations where the local influence is dominant and is shadowing the regional signature. We then need to define the background signal on top of which the regional scale signal is added.

Such local situations and background definitions may be extracted purely from time series analysis procedures, or may be constrained on a physical basis. The main difficulty is to correctly define the baseline signal of the measured time-series and to adequately flag local spikes. El Yazidi et al. (2018) have assessed the efficiency and robustness of three statistical spikes detection methods for CO<sub>2</sub> and CH<sub>4</sub> and have concluded that the two automatic SD and REBS methods could be used after a proper parameters specification. We used the El Yazidi et al. (2018) method on the composite merged minute time series to filter out « spike » situations. From this despiked minute dataset we built hourly means, which were used to analyse the diurnal cycles. Focusing on data with regional footprints, we selected only afternoon data with low hourly variability (estimated from minute standard deviations). We applied the CCGCRV curve fitting program from NOAA (Thoning et al., 1989) to determine the trend and the detrended seasonal cycle of the afternoon means time series for all species. Residuals from the trends and seasonal cycles were then computed.

### 3. Data Quality Assessment

QA/QC protocols are applied at several steps of the measurements system. On a daily basis, a conservative quality control is operated from two complementary sides: On one side, the spectrometers intrinsic properties are verified, and the other one side the sampling system parameters are checked. On a weekly to monthly basis the field spectrometers performances are monitored. A flask program also runs in parallel and is used to expand the atmospheric monitoring to other trace gases but also to assess the quality of the continuous measurements. Up to now, flasks data were not fully available or were contaminated, and thus were not used in the present work. A complementary approach to assess compatibility employs round robin or so-called “cucumbers” cylinders circulated between stations within the ICOS European network. Finally the station compatibility is also assessed during in situ audits using a mobile station and traveling instruments (Hammer et al, 2013, Zellweger et al., 2016).

In this section we used two metrics defined in Yver Kwok et al. (2015) for the quality control assessment of the data. These two metrics are usually calculated under repeatability conditions of measurements where all conditions stay identical over a short period of time. The continuous measurement repeatability (CMR), sometimes called precision, is a repeatability measure applied to continuous measurements. The long-term repeatability (LTR), sometimes called reproducibility, is a repeatability measure over an extended period of time.

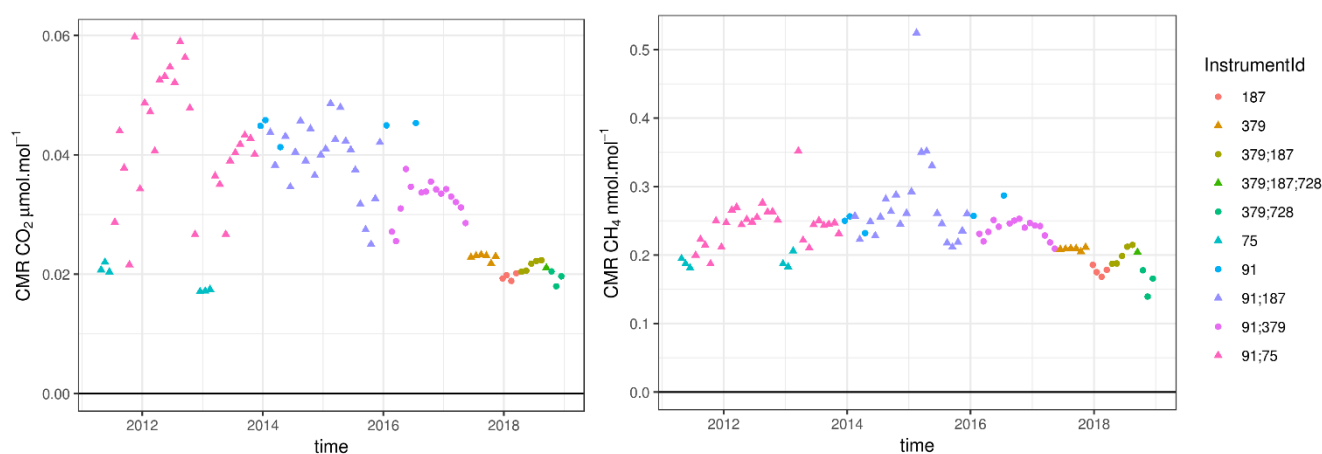
#### 3.1 Short term target quality control: Field continuous measurement repeatability equivalent

In our basic measurements sequence, the air from a high-pressure cylinder (STT) is analysed twice a day with a 10 hours frequency for at least 20 minutes to assess the daily performance of the spectrometers. This metric mainly describes the intrinsic performance of the spectrometers and not of the sampling system. It is a field estimation of the CMR and is computed as the



standard deviations of the raw data over 1 min intervals, the first 10 minutes of each target gas injection being filtered out as stabilisation.

The Figure 5 shows the monthly means CMR of the combined time series of CO<sub>2</sub> and CH<sub>4</sub> using the same type of analysers. The time series of CO's CMR are not shown as the intrinsic properties of the Picarro and Los Gatos Research analysers are very different making it difficult to compare on a same plot. For CO<sub>2</sub>, we observe a decrease of the CMR over the measurement periods, indicating an improvement of the instruments precision. The spectrometer #91 (CRDS, G1301) was shipped to the manufacturer for a major repair including cell replacement between November 2012 and March 2013. The repair at Picarro workshop improved the CMR performance of the analyser from above 0.06 to below 0.05 ppm. For this instrument, the factory estimated a CMR of 0.04 ppm in 2009 and the lab test at ATC MLab in 2012 estimated a CMR of 0.06 ppm.



10

**Figure 5: Monthly mean field Continuous Measurement Repeatability (CMR) for CO<sub>2</sub> (left panel), and CH<sub>4</sub> (right panel) estimated over time for the different instruments in operation at the OPE station over the 2011-2018 period. The different instruments are shown in color and their identifiers are labelled in the legend of the top and bottom panels. Some months, have several instruments running at the station and are identified with several labels**

15 Using a gas chromatograph at the Trainou tall tower, Schmidt et al. (2014) found a mean standard deviation of the hourly target gas injections of 0.14 ppm for CO<sub>2</sub>, 3.2 ppb for CH<sub>4</sub> and 1.9 ppb for CO for the whole period of 2006-2013. Berhanu et al. (2016) presented their system performance using precision, a metric based on the standard deviation of the 1-min target gas measurements, at 0.05ppm for CO<sub>2</sub>, 0.29ppb for CH<sub>4</sub> and 2.79ppb for CO using a Picarro G2400 spectrometer over 19 months from 2013 to 2014. Lopez et al. (2015) presented STR estimates for the gas chromatograph system used at Puy de dôme at 20 0.1ppm for CO<sub>2</sub> and 1.2 ppb for CH<sub>4</sub>, for the years 2010-2013.

The Table 3 presents the comparison of the CO<sub>2</sub> and CH<sub>4</sub> CMR for the instruments #75/91/187/379/728 estimated by the manufacturer, by the ICOS ATC MLab as well as the mean values from the station measurements over the 2011-2018 period. The station performance of each individual analyser is coherent with its performance estimated at the factory and at the ATC MLab. The performances are maintained over several years and were not disturbed by the station settings.

25



Analyser	ICOS Id	CO <sub>2</sub> (ppm)			CH <sub>4</sub> (ppb)		
		factory CMR	ATC Mlab CMR	Field mean CMR	factory CMR	ATC Mlab CMR	Field mean CMR
Picarro G1301	91	0.04	0.059	0.048	0.27	0.24	0.27
Picarro G1301	75	0.019	0.022	0.02	0.18	0.26	0.22
Picarro G2401	187	0.023	0.026	0.021	0.2	0.28	0.22
Picarro G2301	379	0.025	0.023	0.022	0.23	0.22	0.2
Picarro G2401	728	0.014	0.013	0.014	0.1	0.09	0.08

**Table 3: Continuous measurement repeatability (CMR) estimated by the factory, MLab and field means over 2011-2018 of CO<sub>2</sub> (ppm) and CH<sub>4</sub> (ppb). Their model and ICOS Identifier are indicated in the first columns.**

For CH<sub>4</sub>, the factory estimated CMR's for instrument #91 in 2009 was 0.27ppb and the initial lab tests at ATC MLab in 2012 estimated CMR for CH<sub>4</sub> at 0.24 ppb. The repair at Picarro workshop did not modify the CMR performance of the analyser. For each instrument, the CH<sub>4</sub> performance are very stable along the years with very few outliers.

The CO performances (CMR and LTR) estimated at the station are compared to the factory and ATC MLab results in the Table 4.

Analyser	ICOS Id	CO (ppb)				
		factory CMR	ATC Mlab CMR	Field mean CMR	ATC Mlab LTR	Field mean LTR
Los Gatos N <sub>2</sub> O and CO	80	0.15	0.06	0.06	0.3	0.4
Picarro G2401	187	6.5	5.7	5.17	1.7	1.18
Los Gatos	478	0.06	0.09	0.05	0.09	0.05
Picarro G2401	728	2.7	2.69	2.76	0.22	0.33

**Table 4: Continuous measurement repeatability (CMR) and long-term repeatability (LTR) between factory, MLab and field mean over 2011-2018 of CO (ppb). Their model and ICOS Identifier are indicated in the first columns.**

The CO CMR time series (not shown) displays four different periods which are directly linked to the analysers used to build the combined time-series. We used two different analysers type: one build by Los Gatos based on the ICOS technology (instruments #80 and #478) and one build by Picarro based on the CRDS technology (instruments #187 and #728). These two types of analysers have very different internal properties making it difficult to show direct comparison.

Overall the precisions measured at the station for CO<sub>2</sub>, CH<sub>4</sub> and CO remain comparable to the initial values estimated by the manufacturer and the ATC laboratory, showing no degradation due to the design of the station or the measurement procedures.

### 3.2 Short term target quality control: Field long term repeatability

The field LTR is computed as the standard deviation of the averaged STT measurement intervals over 3 days as it is done during the initial test at the ICOS Metrology Lab. Data are then averaged every month. The same STT data as previously are used but with a different perspective, more closely linked to the ambient air data uncertainty.

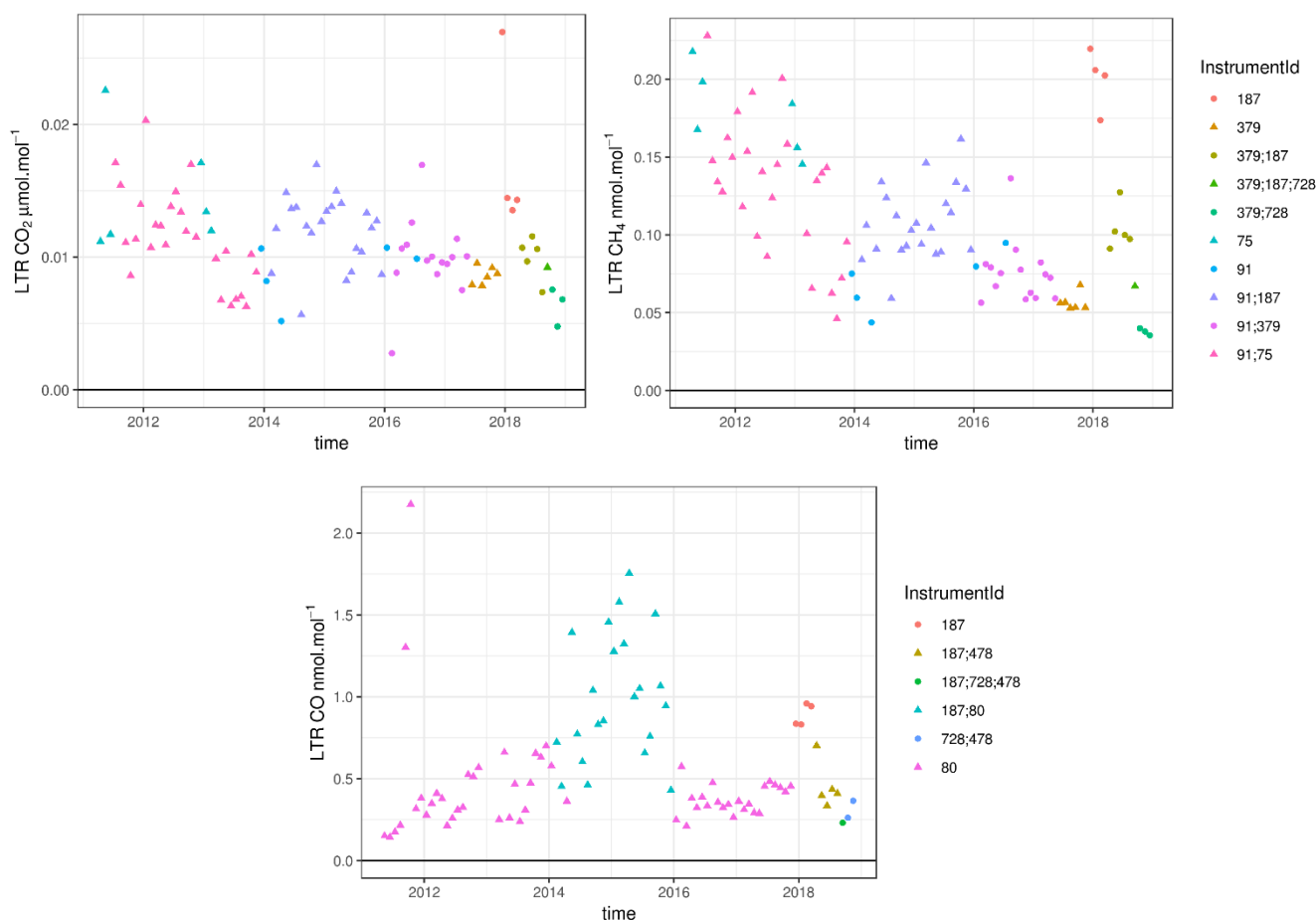


**Figure 6: Monthly mean field long term repeatability (LTR) for CO<sub>2</sub> (top left panel), CH<sub>4</sub> (top right panel) and CO (bottom panel) estimated over time for the different instruments in operation at the OPE station over the 2011-2018 period. The different instruments are shown in colour and their identifiers are labelled in the legend of the top and bottom panels. Some months, have several instruments running at the station and are identified with several labels**

5

The Figure 6 shows the monthly mean field LTR of the merged time series using the different instruments and sampling systems. This figure shows the uncertainties of the data related to the analysers (not the sampling systems). As for CMR, CO<sub>2</sub> and CH<sub>4</sub> LTR show decreasing trends suggesting an improvement of the internal performance of the spectrometers built by Picarro, of the air distribution system as well as data selection/flagging. The beginning part of 2018 experienced a clearly worst LTR compared to neighbouring months. This mostly due to the use of the instrument #187, which have relatively poor performance compared to other instruments.

10



Analyser	ICOS Id	CO <sub>2</sub> (ppm)		CH <sub>4</sub> (ppb)	
		ATC Mlab LTR	Field mean LTR	ATC Mlab LTR	Field mean LTR
Picarro G1301	91	0.02	0.01	0.08	0.08
Picarro G1301	75	0.01	0.01	0.21	0.17
Picarro G2401	187	0.02	0.02	0.22	0.17
Picarro G2301	379	0.007	0.009	0.1	0.06
Picarro G2401	728	0.005	0.008	0.06	0.02

**Table 5: Long term repeatability (LTR) estimated by MLab and field mean over 2011-2018 of CO<sub>2</sub> (ppm) and CH<sub>4</sub> (ppb). Their model and ICOS Identifier are indicated in the first columns**

The comparison of the field mean LTR and ATC MLab LTR for the different instruments are shown on the Table 5 for CO<sub>2</sub> and CH<sub>4</sub>. The LTR field performance of the analysers are in agreement with their initial assessments. Periods of lower CO<sub>2</sub>/CH<sub>4</sub> LTR are associated with instruments #91, #379 or #728 while periods with larger CO<sub>2</sub>/ CH<sub>4</sub> LTR are associated with instruments #75 or #187.

As for CMR, the CO LTR monthly time series shows four different periods but with a smaller contrast, related with the analysers type used at the station. Most periods with LGR instruments (#80 or #478) shows a LTR under 0.7ppb while periods with Picarro instrument #187 shows LTR above 0.5ppb.

Different periods have different uncertainty levels related to the instrument performance. While Los Gatos Research instruments show lower LTR they have stronger temperature sensitivities generating strong short-term variability in conditions where the temperature is not well constrained. Corrections for these temperature induced biases implied the use of a working standard quite frequently

### 15 3.3 Station audit by traveling instruments

A metric such as CMR is very useful to monitor the instrument internal performance and therefore to be able to identify as soon as possible any instrumental failure. Other instrument related metrics such as calibration long term drift or calibration stability over the sequences are also useful to monitor the instrument performance. However, they do not give an assessment of the overall measurement systems. Flask versus in-situ comparisons, or station audit by traveling instruments are recognized as essential tools in the performance and compatibility assessment of a measurement system. The ICOS audits are performed by a mobile lab, hosted by the Finnish Meteorological Institute in Helsinki, and equipped with state of the art GHG analysers and traveling cylinders. The measurements data from the station are centrally processed at the ATC but the data produced by the Mobile Lab, however, are calculated separately to maintain the independent nature of the Mobile Lab and at the same time to evaluate the performance of the centralised data processing.

25 The OPE station was audited two times, once in summer 2011, soon after the station set up, during the feasibility study of the travelling instrument methodology and then in summer 2014, when the ICOS Mobile Lab was ready for operation. During the two weeks intercomparison in 2011, significant differences for CO<sub>2</sub> and CH<sub>4</sub> were noticed between the FTIR traveling



instrument and the CRDS reference instrument (Hammer et al., 2013). As the two instruments have different temporal resolutions and different response times, the CRDS measurements were convoluted with an exponential smoothing kernel representing a 3 min turn-over time to match the FTIR specifications. For CO<sub>2</sub> the smoothed differences vary between 0.1 and 0.2 ppm with a median difference of 0.13 ppm and a scatter of the individual differences on the order of  $\pm 0.15$  ppm. The smoothed CH<sub>4</sub> differences decrease from initially 0.7 ppb to 0.1 ppb, the median difference being 0.4 ppb. Such large differences were caused by relatively poor performances of the CRDS and FTIR instruments because of specific hardware problems but also related to the large temperature variations (10 K) within the measurements container. During the same 2011 summer, the travelling instrument was also set up at the Cabauw (CBW) station in Netherlands. The audit showed better instrument performance but the same kind of differences for ambient air comparisons. While the CO<sub>2</sub> deviations at CBW were partly explained by a travelling instrument intake line drawback and by calibration issues on the main measurements system, at OPE no final explanation for the observed differences have been found.

During summer 2014, the two months audit was performed using a Picarro G2401 travelling instrument as well as a FTIR. Nevertheless the FTIR performance was not yet optimized and the difference of time resolution made it difficult to use properly. Results from this instrument are not considered here. The OPE standard cylinders analysed by the travelling instrument showed on average 0.03 ppm and 0.10 ppm higher CO<sub>2</sub> concentrations in the beginning and in the end of the audit, respectively, than the assigned values used to calibrate measurements at OPE. Similar results were found for CH<sub>4</sub> with relatively low differences ranging between 0 and 1 ppb. The instruments as well as the working standards (OPE and travelling standards) were calibrated against two different standards sets, introducing biases in the measurements of cylinders but also of ambient air. The intercomparison was complicated by the fact that the station was hit by three lightnings during the summer, creating major power outage and electrical damages to the infrastructures. Such power outages generate shifts in the CRDS analyser response that prevent drift correction of the calibration response, degrading the analyser performance. The ambient air comparison was based on two sampling lines, one line supplying a dried Picarro G1301 (#91) and a wet Picarro G2401 (#187), and one independent line for the audit supplying the wet travelling instrument. The wet OPE G2401 data were corrected for water vapour by the factory Picarro correction, but the travelling instrument was corrected by an improved water correction based on water droplet test performed at the beginning of the intercomparison and using a simplified version of Method #2-EMPA implementation presented in Rella et al. (2013). The ambient air mole fractions for CO<sub>2</sub> by both dried and wet OPE analysers showed lower concentrations compared to the wet travelling instrument, by 0.10 ppm at the beginning of the audit, and 0.13 ppm at the end. Most of the differences in ambient air measurements can be explained by the bias in the reference scales.

When averaged over the whole period the OPE minus travelling instrument differences remain within the WMO/GAW component compatibility goal. The dried Picarro G1301 #91 measurements deviated on average by -0.05 ppm compared to the wet Picarro G2401 travelling instrument in the case of CO<sub>2</sub>, and by 0.70 ppb in the case of CH<sub>4</sub>. Similarly the wet Picarro G2401 #187 differs from the travelling instrument by -0.03 ppm and 1.80 ppb for CO<sub>2</sub> and CH<sub>4</sub>, respectively. The comparison

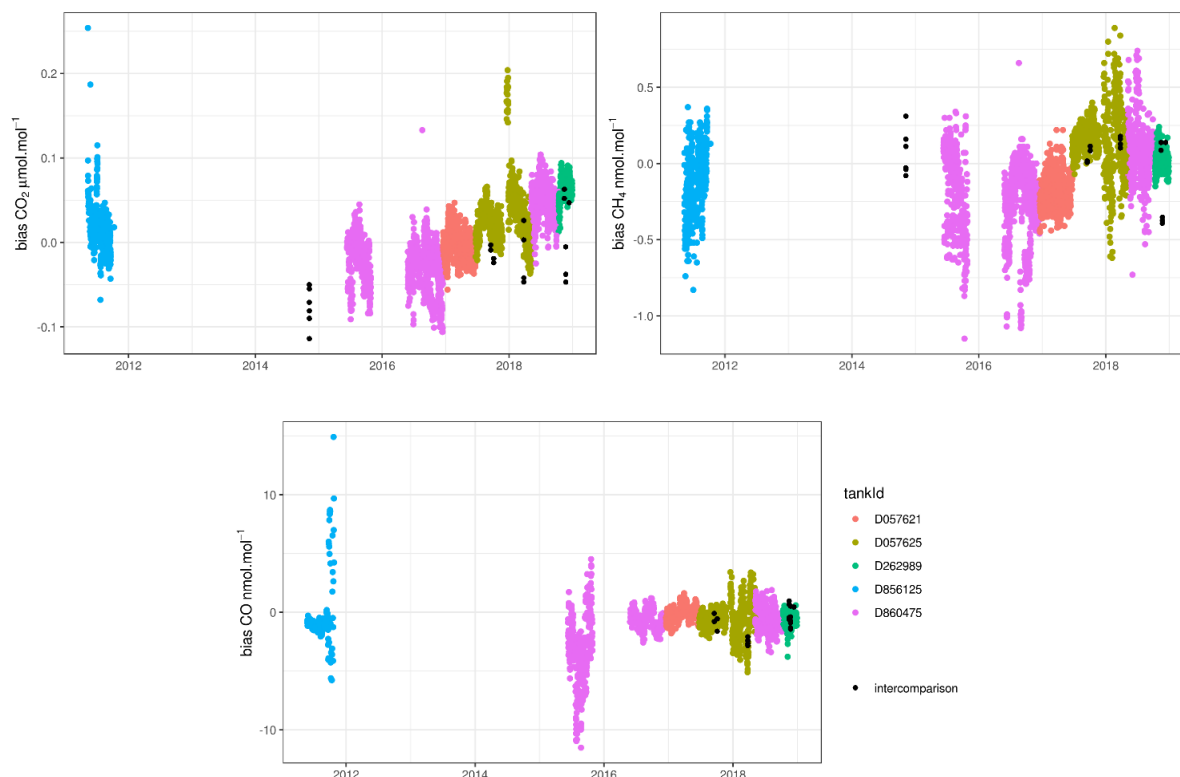




of CO was made for OPE-LGR and OPE-G2401 instruments compared to the travelling instrument G2401: the average deviations were either larger than or barely within the WMO/GAW component compatibility goal ( $\pm 2$  ppb). Vardag et al. (2014) presented similar intercomparison results at Mace Head during two months in spring 2013. For CO<sub>2</sub>, the difference in ambient air measurements at Mace Head between the travelling instrument and the station analyser (Picarro G1301) was  $0.14 \pm 0.04$  ppm. During this intercomparison there was no scale issue as the same scale was used on both system but there could have been also a bias in the water correction effect. Still, most of the differences between the station data and the travelling instrument during ambient air measurements remained unexplained. The present results as well as the previously published results highlight the major difficulties that station PI's are facing with the intercomparison interpretation and understanding. Upcoming sampling line test, mandatory in the ICOS network at least on a yearly basis, may help to understand if the sampling design introduces artefacts.

### 3.4 Travelling “cucumbers” cylinders and station target tank biases

At the beginning of the station operation, quality control tanks, or targets, were not systematically used, neither calibrated. Calibrated tanks were used systematically from 2015 as working standards allowing biases monitoring.



15

**Figure 7** Target tanks biases over time for several tanks for CO<sub>2</sub> (top left panel), CH<sub>4</sub> (top right panel) and CO (bottom panel) in colours. The “cucumbers” intercomparison biases are shown in black. The different colours are related to the different tanks used at the OPE station for quality control.



In addition the station OPE took part to the CarboEurope « cucumber » program in the EURO2 loop at the end of 2014, as well as to the ICOS program started in September 2017. The aims of such programs are to assess the measurement compatibility and quantify potential offsets in calibration scales within a network. The results of these two sequences of « cucumbers » intercomparison are shown on the Figure 7 along with the biases estimated for the station quality control cylinders.

- 5 The biases estimated from the target tanks operated at the station and the blind cucumber intercomparison biases are consistent for all species. CO<sub>2</sub> biases are found between -0.1 and 0.1ppm for most of the times except some outliers that still need to be understood. A trend may be present in the CO<sub>2</sub> biases between 2016 and 2018, not explained. CH<sub>4</sub> biases are between -0.75 and 0.75ppb for most of the cases. CO biases show a large spread at the beginning of the station operation partly related to the temperature sensitivity of the Los Gatos Research analyser and the poor temperature control of the measurements container.
- 10 Since 2016 the CO biases stay within the -5 /+5 ppb range.

#### 4. Results

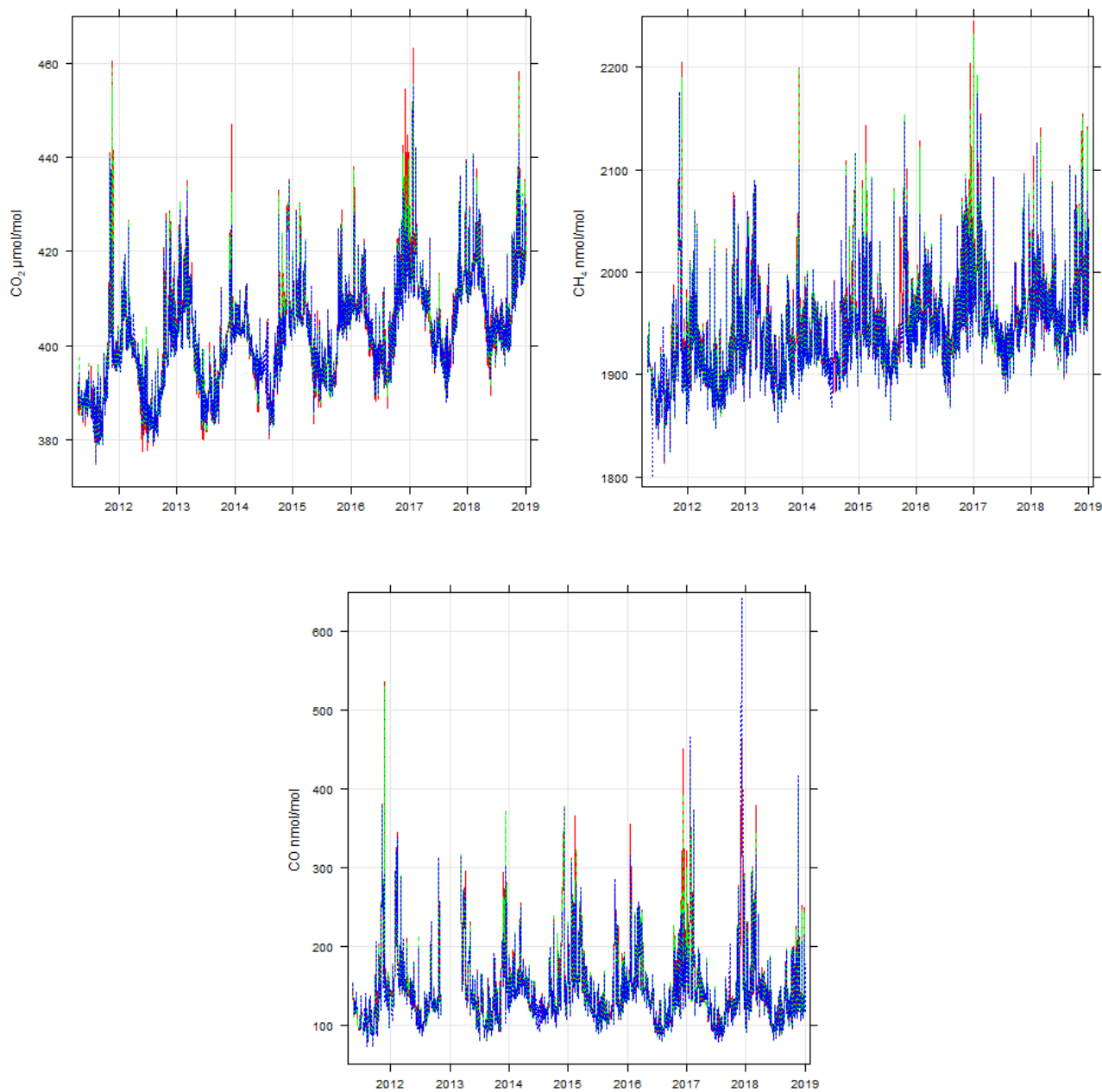
- Tall tower GHG concentration time series over mid latitudes continental areas exhibit strong variations from hourly to weeks, seasons and interannual time scales and even longer. Such variabilities are linked to local, regional and global meteorological variations, as well as land biosphere processes and human activities. After showing the general characteristics of the time series, we will present the diurnal cycles computed from the despiked hourly data. We will then select only stable situations with low fast variability to get a focus on the regional scale and compute afternoon stable means for CO<sub>2</sub>, CH<sub>4</sub>, CO at the three sampling levels.
- 15

##### 4.1 General characteristics of the CO<sub>2</sub>, CH<sub>4</sub>, and CO times series

- The Figure 8 shows the general characteristics of the afternoon means measured mole fractions of CO<sub>2</sub>, CH<sub>4</sub>, CO at the OPE station at the 10m, 50m and 120 m above ground levels. From the summer of 2011 to the end of 2018, the afternoon mean CO<sub>2</sub> at 120m varied from 375 ppm value to a maximum of 455 ppm. A higher variability is recorded at the lowest level (10m) compared to the top level (120m). At 10m the summer minimum concentrations are below the top level concentrations while the winter maximum concentrations are above the top level concentrations. Vertical gradients of CO<sub>2</sub> are present year round but are stronger in summer and weaker in winter, and the gradient variability is also much stronger in summer. During the warm period (from May to September) the mean vertical gradient of CO<sub>2</sub> is 0.4ppm during the afternoon (12:00-17:00 UTC) and -9.95 ppm during the night hours (00:00-05:00 UTC). During the cold period (from October to April) the mean vertical gradient of CO<sub>2</sub> is -0.24 ppm during the afternoon (12:00-17:00 UTC) and -3.5 ppm during the night hours (00:00-05:00 UTC). The CH<sub>4</sub> afternoon mean mole fractions time series are also characterized by a long term trend with a weaker seasonal cycle. Synoptic variations could be as large as 150 to 200 ppb on hourly time scales and are stronger at the lowest level. Vertical gradients of CH<sub>4</sub> are present year round and show a small seasonal cycle. During the warm period the mean vertical gradient of CH<sub>4</sub> is -0.5ppb during the afternoon (12:00-17:00 UTC) and -20.7 ppb during the night hours (00:00-05:00 UTC). During
- 20
- 25
- 30



the cold period (from October to April) the mean vertical gradient of CH<sub>4</sub> is -4 ppb during the afternoon (12:00-17:00 UTC) and -18.5 ppb during the night hours (00:00-05:00 UTC).



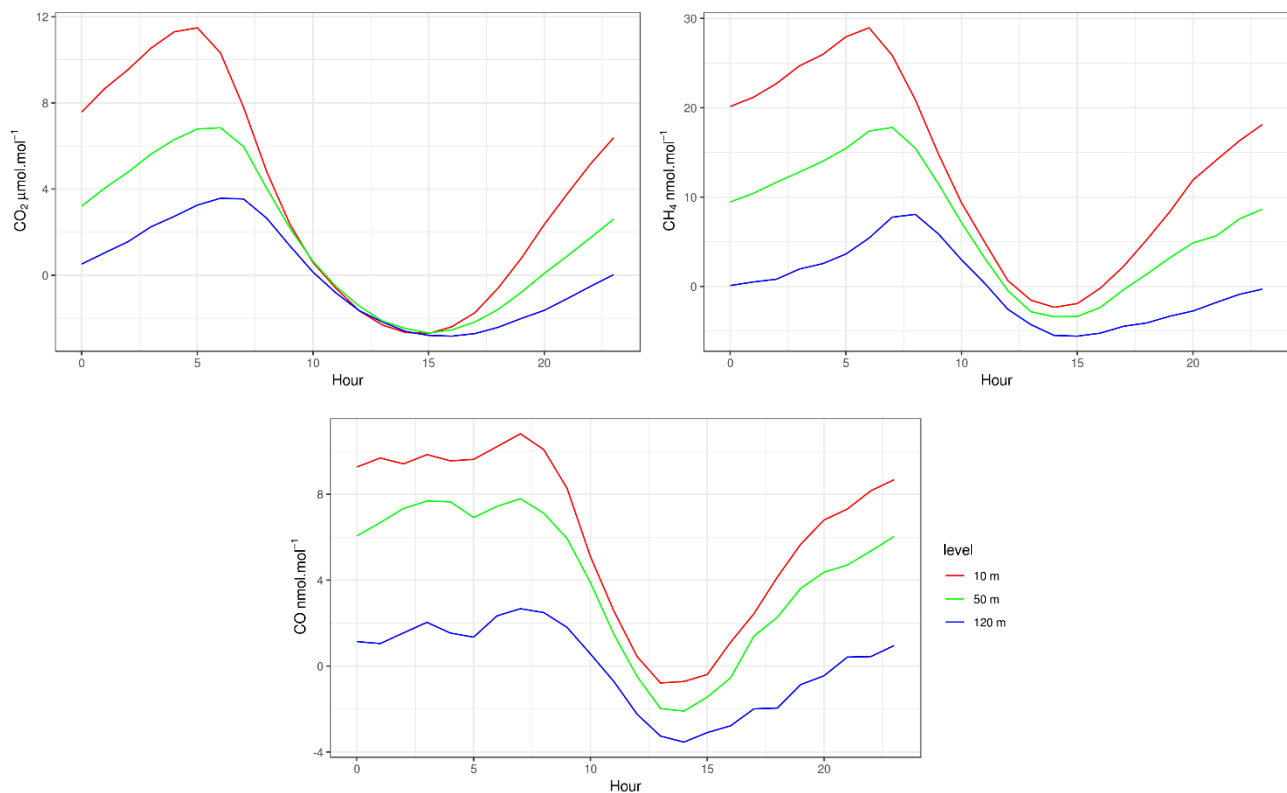
5 **Figure 8:** Afternoon (12:00-17:00 UTC) mean CO<sub>2</sub> (top left panel), CH<sub>4</sub> (top right panel) and CO (bottom panel) mole fractions measured at OPE station at 10m (red), 50m (green) and 120m (blue).



The CO afternoon mean mole fractions time series do not show any long-term trends but are characterized by strong seasonal cycles. Synoptic variations could be as large as 200 ppb on hourly time scales and are stronger at the lowest level. Vertical gradients of CO are much stronger in winter and weaker in summer. The CO lifetime in the atmosphere is strongly related to OH radicals, the major sink, which is seasonally variable. During summer the combined effects of a more active sink, weaker « local » sources and a strong vertical mixing lead to lower concentrations, with smaller variability and weaker vertical gradients. In winter, the OH sink efficiency decreases, local sources are stronger and the meteorological conditions favour non-dispersive situations and weaker vertical mixing leading to higher CO concentrations and stronger vertical gradients.

#### 4.1 Diurnal Cycles

The trace gases diurnal cycles are the results of the atmospheric dynamics (especially the daily amplitude of the boundary layer height), the surface fluxes and the atmospheric chemistry. The mean diurnal cycles of CO<sub>2</sub>, CH<sub>4</sub> and CO are shown on the Figure 9 for the three sampling levels (10m, 50m and 120m).



15 **Figure 9** Mean diurnal cycles of CO<sub>2</sub> (top left panel), CH<sub>4</sub> (top right panel) and CO (bottom panel) for the three sampling levels 10m, 50m and 120m, normalized to the top level 120m, computed over the period 2011-2018.



For the three compounds, the vertical gradients are much stronger during the night, with highest concentrations close to the ground. During daytime, the gradients almost disappear, due to the vertical mixing of the low atmosphere. In spring and summer, the lowest level CO<sub>2</sub> afternoon concentration is slightly below the highest level reflecting the photosynthesis pumping of CO<sub>2</sub> by the vegetation. Vertical gradients build up again in the late afternoon. For CH<sub>4</sub> and CO the vertical gradient stays the same all along the day, the lowest level being higher than the highest levels..

Lags are noticeable between the different levels in the CO<sub>2</sub> and CH<sub>4</sub> diurnal cycle. The night-time peak concentrations occur earlier at the lowest level followed by the intermediate level and then followed by the highest level. The daytime minimum seems to be reached at the same time at the three levels. Then the late afternoon increase is much faster at the lowest level and is also delayed at the highest level. The diurnal cycles of CO<sub>2</sub> and CH<sub>4</sub> are larger in spring and summer while for CO it is larger in winter.

#### 4.2 Data selection and time series analysis

Our aim in this paper is to draw the general behaviours of the major GHG at the station focusing on relatively large scale. We thus focused on stable data discarding situations when local influences could shadow the regional component. We selected afternoon data when the boundary layer is larger and the vertical mixing is more efficient as seen previously. We excluded data showing large variations by using the minute standard deviations. Hourly data with minute standard deviations larger than three interquartile range computed month by month were excluded from the afternoon mean, leading to a rejection of between 2.9 % and 4.2% of the hourly means of the CO<sub>2</sub>, CH<sub>4</sub> and CO.

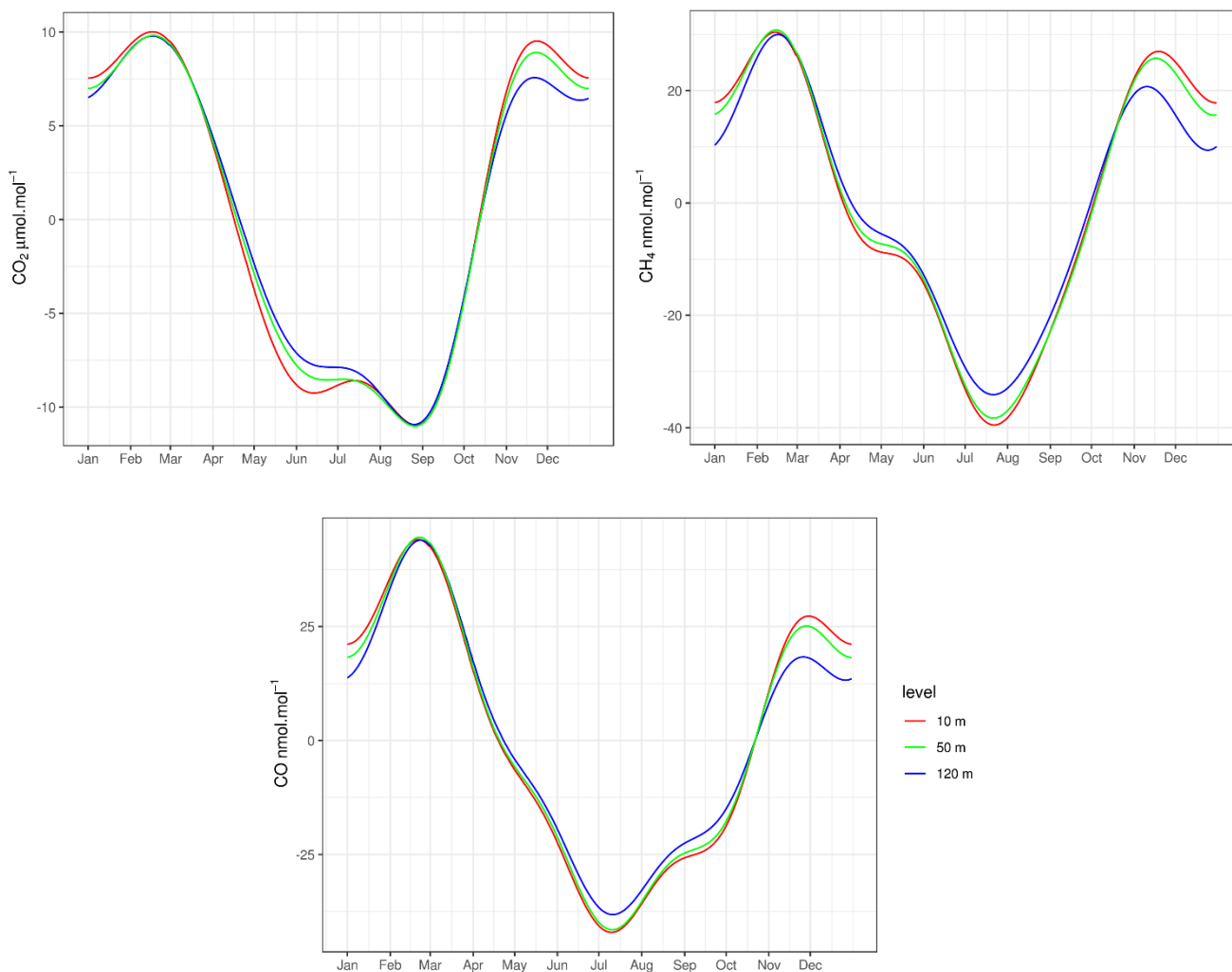
We used the CCGCRV curve fitting program with the standard parameters set (npoly=3, nharm=4) to compute the mean seasonal cycles and trends. CCGCRV results were compared with similar analysis performed with the openair package of R for the seasonal cycle and the trend using the TheilSen method. These seasonal cycle and trend components of the time series are dominated by large-scale processes. In addition strong intra-seasonal variabilities are observed that are related to local and regional scale factors. We computed the residuals from the seasonal cycle and trends using CCGCRV results. We performed a qualitative comparison with residuals computed using the REBS approach which is commonly used to determine the station's background using a statistical approach (not shown). REBS was applied with a bandwidth of 60 days and a maximum of 20 iterations.

#### 4.3 Seasonal cycles

The Figure 10 shows the mean seasonal cycles of the three compounds CO<sub>2</sub>, CH<sub>4</sub> and CO at the three measurement levels (10m, 50m and 120m agl). Each of the three GHG displays a clear seasonal cycle, with higher amplitudes at the lower sampling levels. Minimum values are reached during summer when the boundary layer is higher and the vertical mixing is more efficient. In addition to the boundary layer dynamic, the seasonal cycle of the surface fluxes and the chemical atmospheric sink also play a significant role. The correlations of dynamic and fluxes processes at the seasonal scale make difficult to discriminate the role of each process. Minimum values are reached late summer for CO<sub>2</sub>, around the end of August with no vertical gradients around



this minimum. Vertical gradient appear in the late spring with a maximum gradient in June when a secondary minimum is observed at the lowest level but not at the above levels. CO<sub>2</sub> vertical gradients are also observed late fall - early winter when the lowest level CO<sub>2</sub> is higher than the top level.



5

**Figure 10:** Mean seasonal cycles of the afternoon mean data at the three measurement levels ( 10m in red, 50m in green and 120m in blue) for CO<sub>2</sub> (top left panel), CH<sub>4</sub> (top right panel) and CO (bottom panel) computed over the 2011-2018 period using CCGCRV.

10 Minimum CH<sub>4</sub> values are observed in July and maximum values in February and November. The vertical gradients of CH<sub>4</sub> are stronger in mid-summer and early winter compared to the other seasons. The CO vertical gradients are maximum in November and December. This highlights the enhanced winter anthropogenic emission associated with heating as well as the reduced atmospheric mixing. Large-scale transport may contribute to the increase as emission increases in winter on continental scale. But local activities are also contributing as shown by the stronger vertical gradients and the higher mole



fraction levels near the ground. CO<sub>2</sub> vertical gradients are stronger in November and December, as also shown in the CH<sub>4</sub> and CO vertical gradients, and are weaker from January to April.

#### 4.4 Trends

The Table 6 reports the mean atmospheric growth rates computed for the three compounds at the top level using CCGCRV and TheilSen approaches. Mean CO<sub>2</sub> annual growth rate over the 2011-2018 period is 2.5 ppm/year using TheilSen method and 2.3 ppm/year using CCGCRV. This is in agreement with the Mauna Loa global station rate which is also 2.4 ppm/year on average for the period 2011-2018. It is stronger than the growth rate reported for Zugspitze mountain site: 1.8ppm /year, for 1981-2016 (Yuan et al., 2019), as well as Cabauw: 2.0 ppm/year, over 2005-2009 (Vermeulen et al., 2011).

The mean CH<sub>4</sub> annual growth rate over the 2011-2018 period is 8.8 ppb/year using CCGCRV and 8.9 ppb/year using TheilSen method. It is a bit larger than the annual increase in Globally-Averaged Atmospheric Methane from NOAA which is 7.5 ppb /year over the 2011-2017 period. The CO shows a slightly decreasing non-significant trend at OPE for the period 2011-2018. This finding is consistent with recent observations in Europe and in the US. After a long global decrease since the 1980's, the CO decrease has declined since several years after reaching values below 2 ppm (Lowry et al., 2016, Zellweger et al. 2016).

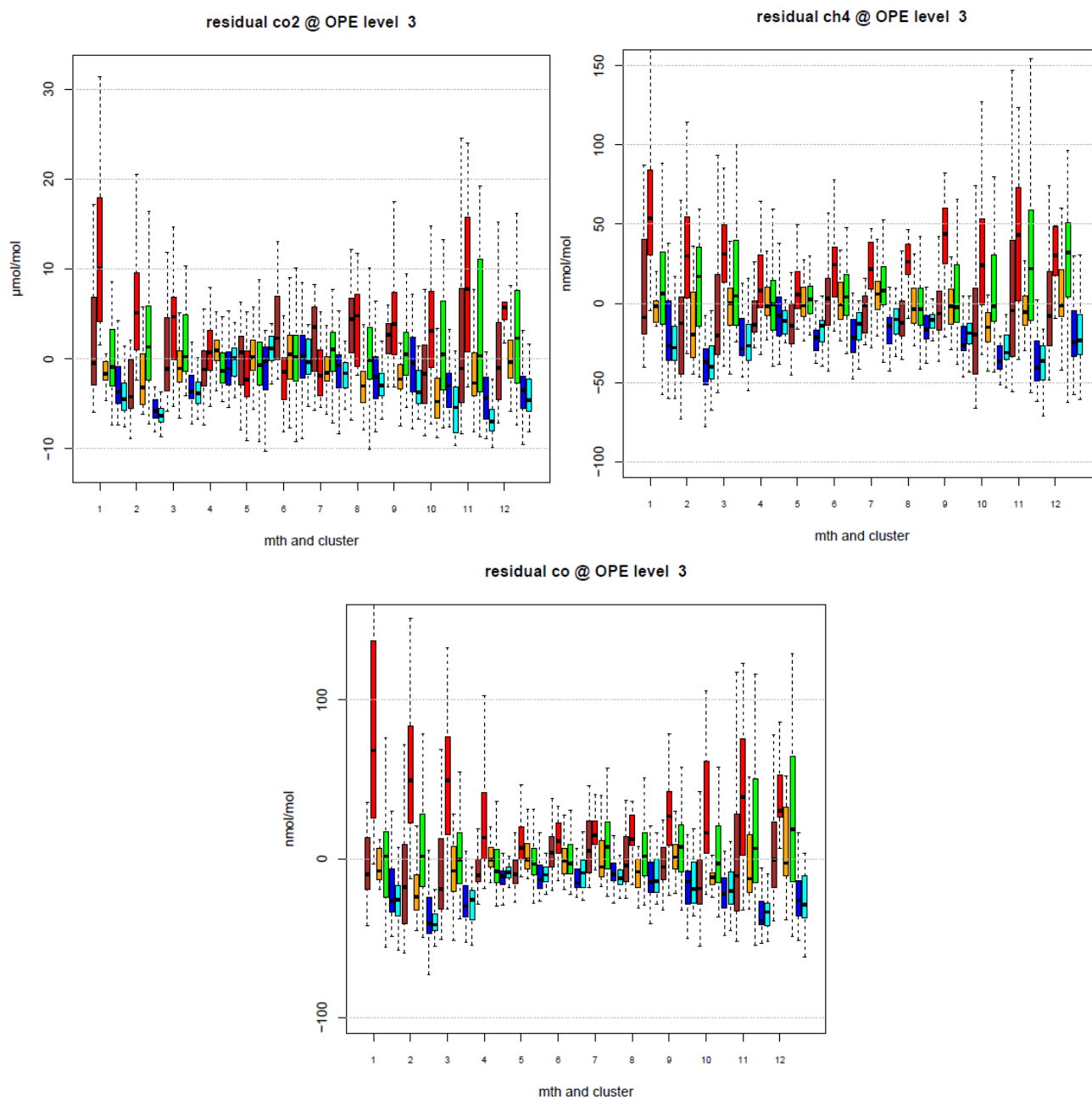
OPE-120m	CO <sub>2</sub> (ppm)	CH <sub>4</sub> (ppb)	CO (ppb)
CCGCRV 2011-2018	2.32	8.83	-0.4
TheilSen2011-2018	2.48	8.86	-0.37

15 **Table 6: Growth rates of CO<sub>2</sub>, CH<sub>4</sub> and CO mole fractions at OPE 120m level for the period 2011-2018 computed on the afternoon mean data using CCGCRV and TheilSen methods.**

#### 4.5 CO<sub>2</sub>, CH<sub>4</sub> and CO residuals

We analysed the residuals from the trend and seasonal cycles fitted curves with regards to air masses back-trajectories using the six clusters defined for the afternoon back trajectories (see Figure 2). The Figure 11 shows the boxplots of the residuals for each month and back-trajectories cluster. The boxplot displays the first and third quartile and the median of the residuals as well as the overall data extension.

The residuals of the three compounds are significantly stronger in the cold months than during the warm months. The clusters 5 (blue colour in Figure 11) and 6 (cyan) are associated with typical oceanic air masses with 96 h back-trajectories reaching far over the Atlantic Ocean. Such air masses are associated with the smallest residuals variability (smallest boxplot extension). Negative residuals are noticed year-round for CH<sub>4</sub> and CO and during the cold months for CO<sub>2</sub> (positive during warm months). Clusters 1 (brown) and 2 (red) are associated with southern and eastern trajectories. The associated residuals are much stronger and show large variabilities among the different synoptic situations with potential large deviations from the background.



5 **Figure 11: Seasonal boxplot of the CO<sub>2</sub> (top left panel), CH<sub>4</sub> (top right panel) and CO residuals (bottom panel) at OPE by cluster occurrence (cluster 1: brown, cluster 2 : red, cluster 3 : orange, cluster 4 : green, cluster 5 : blue, cluster 6 : cyan) for the period 2011-2018**

Positive residuals are noticed for cluster 2 year-round for CH<sub>4</sub> and CO and during the cold months for CO<sub>2</sub>. Cluster 3 (orange) is associated with neutral residuals either negative or positive for the three compounds. Cluster 4 (green) is characterised by relatively "stagnant" air masses with back-trajectories that do not extend far from the station in any particular directions. This





type of air masses is associated with large residuals variability for the three compounds during the cold months. The residuals can be either positive or negative and show large spreads among the situations.

The Table 7 shows the correlation coefficients between the compounds residuals for each back-trajectories cluster, split between a warm period from April to September and a cold period from October to March. During the warm period, the correlation coefficients between CO<sub>2</sub> and either CH<sub>4</sub> or CO are low except for cluster 4. However, the correlation coefficients between CH<sub>4</sub> and CO are around 0.75 for each cluster. During the cold period, the correlation coefficients between the different compounds are high and significant for every type of back-trajectories. Similar seasonal pattern of the CO<sub>2</sub>/CO residuals and CO/CH<sub>4</sub> residuals were shown by Satar et al. (2016) in their two years analysis of the Beromunster tower data in Switzerland.

cluster	1		2		3		4		5		6	
	warm	cold	warm	cold	warm	cold	warm	cold	warm	cold	warm	cold
CO <sub>2</sub> / CH <sub>4</sub>	0.21	0.92	0.33	0.89	0.01	0.84	0.47	0.86	0.18	0.8	0.24	0.87
CO <sub>2</sub> / CO	0.16	0.91	0.4	0.87	0.24	0.85	0.52	0.91	0.24	0.74	0.24	0.78
CH <sub>4</sub> / CO	0.74	0.93	0.87	0.84	0.71	0.87	0.76	0.92	0.75	0.85	0.78	0.88

10 **Table 7 Correlation coefficients between the compounds residuals for each cluster, split between a warm period from April to September and a cold period from October to March.**

Such patterns suggest that, during the cold months, the three compounds fluctuations are associated with the same anthropogenic processes convoluted through the atmospheric dispersion. However, during the warm months CO<sub>2</sub> residuals intraseasonal variations may have different drivers than CO or CH<sub>4</sub> residuals or scale footprints are different. For example natural biospheric contributions from different scales (local to continental) are larger for CO<sub>2</sub> during the warm months. Photochemical reactions are also much more activated. This is suggesting that biospheric CO<sub>2</sub> fluxes may be the dominant driver of CO<sub>2</sub> intraseasonal variations during the warm period while anthropogenic emissions are leading the intraseasonal variations of the three compounds during the cold period.

## 5. Conclusion

The OPE station is a new atmospheric station that was set up in 2011 as part of the ICOS Demo Experiment. It is a continental station sampling air-masses influenced within regional footprints. In addition to greenhouse gases and meteorological parameters mandatory for ICOS, the station is measuring aerosol properties, radioactivity and is part of the regional air quality network. The greenhouse gases measurements are performed in compliance with the ICOS atmospheric station specifications, and it was labelled as part of ICOS-ERIC in 2017. We presented the GHG measurement system as well as the quality control performed. Then analysis of the diurnal cycle, seasonal cycles and trends were shown for the GHG data over the period 2011-2018. Lastly we analysed the compounds residuals with regards to the air masses history.

The monthly mean field CMR were estimated between 0.01 and 0.04 ppm for CO<sub>2</sub>, 0.14 and 0.5 ppb for CH<sub>4</sub> and 0.1 and 5.4 ppb for CO. The monthly mean field LTR were estimated between 0.003 and 0.013 ppm for CO<sub>2</sub>, between 0.03 and 0.23 ppb



for CH<sub>4</sub>, and between 0.14 and 2.17ppb for CO. Biases estimated from the station working standards or by the cucumbers intercomparison are between ±0.1 ppm for CO<sub>2</sub>, ±0.75 ppb for CH<sub>4</sub> and ±5 ppb for CO since 2016.

The station was audited two times, once just after its start in 2011 and then in 2014. In 2011, the field audit revealed a median difference of 0.13 ppm for CO<sub>2</sub> and of 0.4 ppb for CH<sub>4</sub>. During the 2014 audit, the mean biases were between 0.03 and 0.05  
5 ppm for CO<sub>2</sub> and between 0.7 and 1.8 ppb for CH<sub>4</sub>.

The diurnal cycles of the three compounds show the amplification of the vertical gradient during the night mainly caused by the night-time boundary layer stratification associated with the ground cooling and the radiative loss. Minimum values are reached during daytime when the vertical mixing is more efficient. In addition to this main atmospheric dynamics influence, diurnal cycles of the surface emissions and of the chemical processes are also playing some roles in the diurnal profiles of the  
10 three compounds. Interested on larger scale processes we focus on the afternoon data. We computed the mean seasonal cycles of CO<sub>2</sub>, CH<sub>4</sub> and CO. In addition quite strong positive trends were observed for CO<sub>2</sub> and CH<sub>4</sub> with a mean annual growth rate of 2.4 ppm/year and 8.8 ppb/year respectively for the period 2011-2018. No significant trend was observed for CO.

The residuals from the trends and seasonal cycles identified by the time series decompositions are much stronger during the cold period (October to March ) than during the warm period (April to September.) Our analysis of the residuals highlights the  
15 major influence of the air masses on the atmospheric compositions residuals. Air masses originating from the western quadrant with an Atlantic Ocean signature are associated with the lowest residual variability. Eastern continental air masses or stagnant situations are associated with larger residuals and large variability. The correlations between the compounds residuals are also stronger during the cold period. Furthermore, there are no significant correlation between CO<sub>2</sub> and CO or CH<sub>4</sub> during the warm period. This is reflecting that summer CO<sub>2</sub> residuals have important natural sources while anthropogenic drivers dominate CO  
20 and CH<sub>4</sub> variations.

## Acknowledgements

The authors gratefully acknowledge the NOAA Air Resources Laboratory (ARL) for the provision of the HYSPLIT transport and dispersion model and/or READY website (<http://www.ready.noaa.gov>) used in this publication. S. Hammer from  
25 Heidelberg University and H. Aaltonen from FMI are thanked for their efforts during the OPE station audits. Staff from IRFU-CEA are acknowledged for their contribution to the station initial design and installation. We also thank staff from SNO-ICOS-France and from the ICOS Atmospheric Thematic Center for their technical support.

**Competing interests:** The authors declare that they have no conflict of interest.

30



## References

- Bergamaschi, P., Karstens, U., Manning, A. J., Saunois, M., Tsuruta, A., Berchet, A., Vermeulen, A. T., Arnold, T., Janssens-Maenhout, G., Hammer, S., Levin, I., Schmidt, M., Ramonet, M., Lopez, M., Lavric, J., Aalto, T., Chen, H., Feist, D. G., Gerbig, C., Haszpra, L., Hermansen, O., Manca, G., Moncrieff, J., Meinhardt, F., Necki, J., Galkowski, M., O'Doherty, S.,  
5 Paramonova, N., Scheeren, H. A., Steinbacher, M., and Dlugokencky, E.: Inverse modelling of European CH<sub>4</sub> emissions during 2006–2012 using different inverse models and reassessed atmospheric observations, *Atmos. Chem. Phys.*, 18, 901-920, <https://doi.org/10.5194/acp-18-901-2018>, 2018
- Berhanu, T. A., Satar, E., Schanda, R., Nyfeler, P., Moret, H., Brunner, D., Oney, B., and Leuenberger, M.: Measurements of  
10 greenhouse gases at Beromünster tall-tower station in Switzerland, *Atmos. Meas. Tech.*, 9, 2603-2614, <https://doi.org/10.5194/amt-9-2603-2016>, 2016
- Broquet, G., Chevallier, F., Bréon, F.-M., Kadyrov, N., Alemanno, M., Apadula, F., Hammer, S., Haszpra, L., Meinhardt, F., Morguá, J. A., Necki, J., Piacentino, S., Ramonet, M., Schmidt, M., Thompson, R. L., Vermeulen, A. T., Yver, C., and Ciais,  
15 P.: Regional inversion of CO<sub>2</sub> ecosystem fluxes from atmospheric measurements: reliability of the uncertainty estimates, *Atmos. Chem. Phys.*, 13, 9039-9056, <https://doi.org/10.5194/acp-13-9039-2013>, 2013.
- El Yazidi, A., Ramonet, M., Ciais, P., Broquet, G., Pison, I., Abbaris, A., Brunner, D., Conil, S., Delmotte, M., Gheusi, F., Guerin, F., Hazan, L., Kachroudi, N., Kouvarakis, G., Mihalopoulos, N., Rivier, L., and Serça, D.: Identification of spikes  
20 associated with local sources in continuous time series of atmospheric CO, CO<sub>2</sub> and CH<sub>4</sub>, *Atmos. Meas. Tech.*, 11, 1599-1614, <https://doi.org/10.5194/amt-11-1599-2018>, 2018.
- Hammer, S., Konrad, G., Vermeulen, A. T., Laurent, O., Delmotte, M., Jordan, A., Hazan, L., Conil, S., and Levin, I.: Feasibility study of using a "travelling" CO<sub>2</sub> and CH<sub>4</sub> instrument to validate continuous in situ measurement stations, *Atmos.  
25 Meas. Tech.*, 6, 1201-1216, <https://doi.org/10.5194/amt-6-1201-2013>, 2013
- Hazan, L., Tarniewicz, J., Ramonet, M., Laurent, O., and Abbaris, A.: Automatic processing of atmospheric CO<sub>2</sub> and CH<sub>4</sub> mole fractions at the ICOS Atmosphere Thematic Centre, *Atmos. Meas. Tech.*, 9, 4719-4736, <https://doi.org/10.5194/amt-9-4719-2016>, 2016  
30
- Kadyrov, N., Broquet, G., Chevallier, F., Rivier, L., Gerbig, C., and Ciais, P.: On the potential of the ICOS atmospheric CO<sub>2</sub> measurement network for estimating the biogenic CO<sub>2</sub> budget of Europe, *Atmos. Chem. Phys.*, 15, 12765-12787, <https://doi.org/10.5194/acp-15-12765-2015>,



- Kountouris, P., Gerbig, C., Rödenbeck, C., Karstens, U., Koch, T. F., and Heimann, M.: Atmospheric CO<sub>2</sub> inversions on the mesoscale using data-driven prior uncertainties: quantification of the European terrestrial CO<sub>2</sub> fluxes, *Atmos. Chem. Phys.*, 18, 3047-3064, <https://doi.org/10.5194/acp-18-3047-2018>, 2018
- 5 Kromer B., Münnich K.O.: Co<sub>2</sub> Gas Proportional Counting in Radiocarbon Dating — Review and Perspective. In: Taylor R.E., Long A., Kra R.S. (eds) *Radiocarbon After Four Decades*. Springer, New York, NY, 1992
- Laurent, O.: ICOS Atmospheric Station Specifications, ICOS technical report (publicly available on [https://icos-atc.lsce.ipsl.fr/doc\\_public](https://icos-atc.lsce.ipsl.fr/doc_public)), 2017
- 10 Le Quéré, C. and coauthors: Global Carbon Budget 2018, *Earth System Science Data*, 10, 1-54, 2018, DOI: 10.5194/essd-10-2141-2018
- 15 Lebeque, B., Schmidt, M., Ramonet, M., Wastine, B., Yver Kwok, C., Laurent, O., Belviso, S., Guemri, A., Philippon, C., Smith, J., and Conil, S.: Comparison of nitrous oxide (N<sub>2</sub>O) analyzers for high-precision measurements of atmospheric mole fractions, *Atmos. Meas. Tech.*, 9, 1221-1238, <https://doi.org/10.5194/amt-9-1221-2016>, 2016
- Leip A, Skiba U, Vermeulen A, Thompson RL.: A complete rethink is needed on how greenhouse gas emissions are quantified for national reporting. *Atmospheric Environment*. 174:237-240. <https://doi.org/10.1016/j.atmosenv.2017.12.006>; 2018
- 20 Levin, I., Münnich, K., Weiss, W.: The Effect of Anthropogenic CO<sub>2</sub> and <sup>14</sup>C Sources on the Distribution of <sup>14</sup>C in the Atmosphere. *Radiocarbon*, 22(2), 379-391. doi:10.1017/S003382220000967X, 1980
- 25 Lopez, M., Schmidt, M., Ramonet, M., Bonne, J.-L., Colomb, A., Kazan, V., Laj, P., and Pichon, J.-M.: Three years of semicontinuous greenhouse gas measurements at the Puy de Dôme station (central France), *Atmos. Meas. Tech.*, 8, 3941-3958, <https://doi.org/10.5194/amt-8-3941-2015>, 2015
- Lowry, D. et al. Marked long-term decline in ambient CO mixing ratio in SE England, 1997–2014: evidence of policy success in improving air quality. *Sci. Rep.* 6, 25661; doi: 10.1038/srep25661, 2016
- 30



- Nisbet, E. G., Manning, M. R., Dlugokencky, E. J., Fisher, R. E., Lowry, D., Michel, S. E., et al: Very strong atmospheric methane growth in the 4 years 2014–2017: Implications for the Paris Agreement. *Global Biogeochemical Cycles*, 33. <https://doi.org/10.1029/2018GB006009>, 2019
- 5 Peters, G. P., Le Quéré, C., Andrew, R. M., Canadell, J. G., Friedlingstein, P., Ilyina, T., Jackson, R. B., Joos, F., Korsbakken, J. I., McKinley, G. A., Sitch, S., and Tans, P.: Towards real-time verification of CO<sub>2</sub> emissions, *Nat. Clim. Change*, 7, 848–850, <https://doi.org/10.1038/s41558-017-0013-9>, 2017
- Pison, I., Berchet, A., Saunois, M., Bousquet, P., Broquet, G., Conil, S., Delmotte, M., Ganesan, A., Laurent, O., Martin, D.,  
10 O'Doherty, S., Ramonet, M., Spain, T. G., Vermeulen, A., and Yver Kwok, C.: How a European network may help with estimating methane emissions on the French national scale, *Atmos. Chem. Phys.*, 18, 3779–3798, <https://doi.org/10.5194/acp-18-3779-2018>, 2018
- Rella, C. W., Chen, H., Andrews, A. E., Filges, A., Gerbig, C., Hatakka, J., Karion, A., Miles, N. L., Richardson, S. J.,  
15 Steinbacher, M., Sweeney, C., Wastine, B., and Zellweger, C.: High accuracy measurements of dry mole fractions of carbon dioxide and methane in humid air, *Atmos. Meas. Tech.*, 6, 837–860, <https://doi.org/10.5194/amt-6-837-2013>, 2013
- Satar, E., Berhanu, T. A., Brunner, D., Henne, S., and Leuenberger, M.: Continuous CO<sub>2</sub>/CH<sub>4</sub>/CO measurements (2012–2014) at Beromünster tall tower station in Switzerland, *Biogeosciences*, 13, 2623–2635, <https://doi.org/10.5194/bg-13-2623-2016>,  
20 2016
- Schibig, M. F., Steinbacher, M., Buchmann, B., van der Laan-Luijkx, I. T., van der Laan, S., Ranjan, S., and Leuenberger, M. C.: Comparison of continuous in situ CO<sub>2</sub> observations at Jungfraujoch using two different measurement techniques, *Atmos. Meas. Tech.*, 8, 57–68, <https://doi.org/10.5194/amt-8-57-2015>, 2015  
25
- Schmidt, M., Lopez, M., Yver Kwok, C., Messenger, C., Ramonet, M., Wastine, B., Vuillemin, C., Truong, F., Gal, B., Parmentier, E., Cloué, O., and Ciais, P.: High-precision quasi-continuous atmospheric greenhouse gas measurements at Trainou tower (Orléans forest, France), *Atmos. Meas. Tech.*, 7, 2283–2296, <https://doi.org/10.5194/amt-7-2283-2014>, 2014
- 30 Thoning, K.W., P.P. Tans, and W.D. Komhyr, Atmospheric carbon dioxide at Mauna Loa Observatory, 2. Analysis of the NOAA/GMCC data, 1974–1985., *J. Geophys. Res.*, 94, 8549–8565, 1989



- Vardag, S. N., Hammer, S., O'Doherty, S., Spain, T. G., Wastine, B., Jordan, A., and Levin, I.: Comparisons of continuous atmospheric CH<sub>4</sub>, CO<sub>2</sub> and N<sub>2</sub>O measurements – results from a travelling instrument campaign at Mace Head, Atmos. Chem. Phys., 14, 8403-8418, <https://doi.org/10.5194/acp-14-8403-2014>, 2014
- 5 Turner, A.J., Frankenberg, C., Kort, E.A.: Interpreting contemporary trends in atmospheric methane, Proc. Natl. Acad. Sci., 116 (8) 2805-2813; DOI: 10.1073/pnas.1814297116, 2019
- Vermeulen, A. T., Hensen, A., Popa, M. E., van den Bulk, W. C. M., and Jongejan, P. A. C.: Greenhouse gas observations from Cabauw Tall Tower (1992–2010), Atmos. Meas. Tech., 4, 617-644, <https://doi.org/10.5194/amt-4-617-2011>, 2011
- 10 Yuan, Y., Ries, L., Petermeier, H., Trickl, T., Leuchner, M., Couret, C., Sohmer, R., Meinhardt, F., and Menzel, A.: On the diurnal, weekly, and seasonal cycles and annual trends in atmospheric CO<sub>2</sub> at Mount Zugspitze, Germany, during 1981–2016, Atmos. Chem. Phys., 19, 999-1012, <https://doi.org/10.5194/acp-19-999-2019>, 2019
- Yver Kwok, C., Laurent, O., Guemri, A., Philippon, C., Wastine, B., Rella, C. W., Vuillemin, C., Truong, F., Delmotte, M.,
- 15 Kazan, V., Darding, M., Lebègue, B., Kaiser, C., Xueref-Rémy, I., and Ramonet, M.: Comprehensive laboratory and field testing of cavity ring-down spectroscopy analyzers measuring H<sub>2</sub>O, CO<sub>2</sub>, CH<sub>4</sub> and CO, Atmos. Meas. Tech., 8, 3867-3892, <https://doi.org/10.5194/amt-8-3867-2015>, 2015.
- Zellweger, C., Emmenegger, L., Firdaus, M., Hatakka, J., Heimann, M., Kozlova, E., Spain, T. G., Steinbacher, M., van der
- 20 Schoot, M. V., and Buchmann, B.: Assessment of recent advances in measurement techniques for atmospheric carbon dioxide and methane observations, Atmos. Meas. Tech., 9, 4737-4757, <https://doi.org/10.5194/amt-9-4737-2016>, 2016